JOC The Journal of Organic Chemistry

ARTICLE

pubs.acs.org/joc

Synthesis and Characterization of Conformationally Preorganized, (*R*)-Diethylene Glycol-Containing γ-Peptide Nucleic Acids with Superior Hybridization Properties and Water Solubility

Bichismita Sahu, Iulia Sacui, Srinivas Rapireddy, Kimberly J. Zanotti, Raman Bahal, Bruce A. Armitage, and Danith H. Ly*

Department of Chemistry and Center for Nucleic Acids Science and Technology (CNAST), Carnegie Mellon University, 4400 Fifth Avenue, Pittsburgh, Pennsylvania 15213, United States

Supporting Information

ABSTRACT: Developed in the early 1990s, peptide nucleic acid (PNA) has emerged as a promising class of nucleic acid mimic because of its strong binding affinity and sequence selectivity toward DNA and RNA and resistance to enzymatic degradation by proteases and nucleases; however, the main drawbacks, as compared to other classes of oligonucleotides, are water solubility and biocompatibility. Herein we show that installation of a relatively small, hydrophilic (*R*)-diethylene glycol ("miniPEG", *R*-MP) unit at the γ-backbone transforms a randomly folded PNA into a right-handed helix. Synthesis of optically pure $^{R\text{-MP}}\gamma$PNA monomers is described, which can be accomplished in a few simple steps from a commercially available and relatively cheap Boc-L-serine. Once synthesized, $^{R\text{-MP}}\gamma$PNA oligomers are preorganized into a right-handed helix, hybridize to DNA and RNA with greater affinity and sequence selectivity, and are more water soluble and less aggregating than the parental PNA oligomers. The results presented herein have important implications for the future design and application of PNA in biology, biotechnology, and medicine, as well as in other disciplines, including drug discovery and molecular engineering.

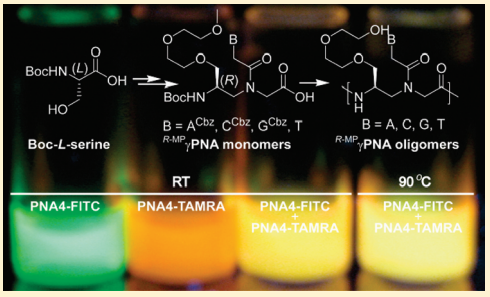

INTRODUCTION

Peptide nucleic acid (PNA) is a promising class of nucleic acid mimic developed in the past two decades in which the naturally occurring sugar phosphodiester backbone is replaced with *N*-(2-aminoethyl)glycine units (Chart 1).[1] PNA can hybridize to cDNA or RNA just as the natural counterpart, in accordance with the Watson−Crick base-pairing rules, but with higher affinity and sequence selectivity.[2] Furthermore, PNA can invade selected sequences of double-stranded DNA (dsDNA).[3−5] The improvement in thermodynamic stability has been attributed, in part, to the lack of electrostatic repulsion in the backbone.[1] The other contribution may come from counterion release upon hybridization, as opposed to condensation taking place with DNA and RNA, resulting in an increase in the overall entropy of the system.[6] The enhancement in sequence selectivity, however, is less well understood.[7] Structural studies suggested that hydration may play a key role in rigidifying the backbone of PNA upon hybridization to DNA or RNA (or PNA), making it less accommodating to structural mismatches. Structural or spinal water molecules have been observed in the X-ray structures of PNA−DNA[8] and PNA−PNA[9−11] duplexes bridging the amide proton in the backbone to the adjacent nucleobase. Besides hybridization properties, another appealing aspect of PNA is enzymatic stability. Because of its unnatural backbone, PNA is not easily degraded by proteases or nucleases.[12] These properties, along with the ease[13,14] and flexibility[15] of synthesis, together make PNA an attractive reagent for many applications in biology, biotechnology, and medicine.[16,17]

PNA has so far been employed in a number of applications, from molecular tools for probing and manipulating nucleic acid structures and functions[18−21] and regulation of gene expression[22,23] to the recognition code for tagging molecules in drug discovery,[24,25] amplifying genetic information in molecular evolution,[26,27] and organizing molecular self-assembly in materials science and nanotechnology.[28−32] In spite of its many appealing features, however, PNA has one major setback as compared to other classes of oligonucleotides. Because of the charge-neutral backbone, PNA is only moderately soluble in aqueous solution. Furthermore, it has a tendency to aggregate and adhere to surfaces and other macromolecules in a nonspecific manner.[33,34] This inherent property posts a considerable technical challenge for the handling and processing of PNA—for instance, in the development of microarrays and related surface-bound applications, because of its propensity to aggregate and collapse onto the surface, causing poor and nonspecific binding,[35,36] and in biology and medicine, in part because of the concerns for off-target binding and cytotoxicity.[34]

In attempts to address this concern, several approaches have been taken, including incorporation of charged amino acid

Received: March 18, 2011
Published: May 27, 2011

Chart 1. Chemical Structures of DNA (RNA), PNA, and MP-Containing γPNA Units

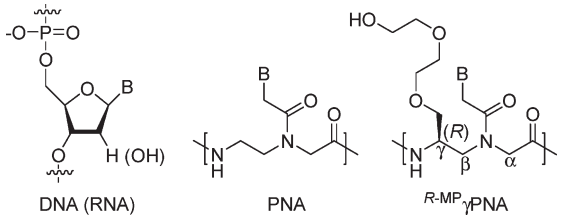

residues, such as lysine at the termini[37] or in the interior part of the oligomer,[38,39] inclusion of polar groups in the backbone,[40] carboxymethylene bridge,[41] and nucleobases,[25,42] replacement of the original (aminoethyl)glycyl backbone skeleton with a negatively charged scaffold,[43,44] conjugation of high molecular weight polyethylene glycol (PEG) to one of the termini,[36,45] fusion of PNA to DNA to generate a chimeric oligomer,[46−50] and redesign of the backbone architecture.[51] These chemical modifications have led to improvement in solubility, but it is often achieved at the expense of binding affinity and/or sequence specificity, not to mention the requirement of an elaborate synthetic scheme in some cases. Incorporation of cationic residues can improve water solubility, but it can also lead to nonspecific binding due to an increase in charge−charge interaction upon hybridization to DNA or RNA. Conjugation of PNA to DNA (or RNA) can improve water solubility as well, but it can compromise binding affinity due to an increase in charge−charge repulsion and conformational heterogeneity in the backbone.[46,47,49] Herein we report the development of a new class of conformationally preorganized, diethylene glycol-containing γPNAs that exhibit superior hybridization properties and water solubility as compared to the original PNA design or any other chiral γPNA that has been developed to date.

RESULTS AND DISCUSSION

Design Rationale. Diethylene glycol, commonly referred to as "miniPEG" or MP, was chosen as a chemical moiety for incorporation in the backbone of PNA because of its relatively small size and hydrophilic nature and the fact it has been shown to be nontoxic and nonimmunogenic.[52−54] MP and larger molecular weight PEG have been incorporated into a number of macromolecular systems, including peptides and proteins,[55] nucleic acids,[45,56−60] carbohydrates,[61] synthetic polymers,[62] dendrimers,[63] liposomes,[64,65] nanoparticles,[66,67] and self-assembled materials,[68] just to name a few, in attempts to improve their aqueous solubility, enzymatic stability, bioavailability, and pharmacokinetics as well as to minimize their immunogenicity. Incorporation of MP into the backbone of PNA is expected to confer similar beneficial effects, including improvements in water solubility and biocompatibility, along with reduction in aggregation and nonspecific binding. Inspection of the PNA backbone reveals three obvious sites for incorporation of this chemical moiety—α, β, and γ (Chart 1). We selected the γ-position because prior studies from our group[69−73] have revealed that installation of a chiral center at this position induces helical organization in the oligomer, providing an additional means for fine-tuning the thermodynamic stability of PNA. γPNAs have been made by other groups before, but their emphasis has been mainly on synthesis[74−77] and covalent attachment of PNA to other functional groups or molecular entities.[78−80]

Scheme 1. Synthesis of $^{R\text{-}MP}$γPNA Monomers[a]

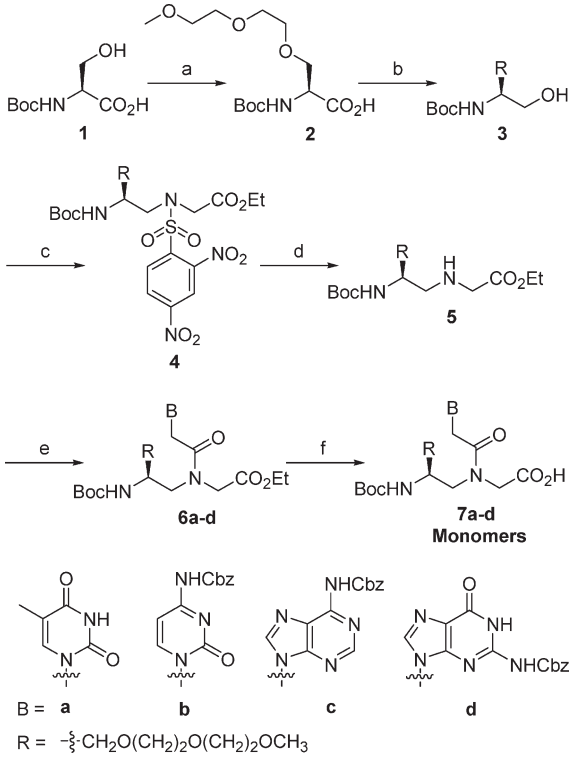

[a] Reagents and conditions: (a) NaH, $BrCH_2CH_2OCH_2CH_2OCH_3$, DMF, 0 °C, 68%; (b) isobutyl chloroformate, $NaBH_4$, NMM, DME, 0 °C → rt, 84%; (c) DIAD, [(2,4-dinitrophenyl)sulfonyl]glycine ethyl ester, TPP, THF, 0 °C → rt, 56%; (d) *n*-propylamine, CH_2Cl_2, rt, 81%; (e) carboxymethylene nucleobase, DCC, DhbtOH, DMF, 50 °C, 67−85%; (f) 2 M NaOH/THF (1:1), 0 °C, 85−98%.

The helical sense, i.e., whether it adopts a right-handed or left-handed helix, is determined by the stereochemistry. γPNAs prepared from L-amino acids adopt a right-handed helix, while those prepared from D-amino acids adopt a left-handed helix; however, only the right-handed helical γPNAs hybridize to DNA and RNA with high affinity and sequence selectivity. Furthermore, we showed that the fully modified, L-alanine-derived γPNAs ($^{S\text{-}Ala}$γPNAs) can invade mixed-sequence double-helical B-form DNA (B-DNA).[81] Though they are promising as antisense and antigene reagents, $^{S\text{-}Ala}$γPNAs are poorly soluble in water and have a tendency to aggregate, presumably due to the charge-neutral backbone and hydrophobic character of the methyl group at the γ-backbone position. We surmised that replacement of the methyl group with MP might ameliorate some of these issues while maintaining the superior hybridization properties of the original γPNA design because of the helical preorganization in the backbone upon installation of MP at the γ-position (Chart 1).

Monomer Synthesis. Boc-protected $^{R\text{-}MP}$γPNA monomers containing all four natural nucleobases (A, C, G, T) were synthesized according to the procedures outlined in Scheme 1. Alkylation of Boc-protected L-serine (**1**) with 1-bromo-2-(2-methoxyethoxy)ethane under an optimized reaction condition: slow addition of **1** into a vigorously stirred, chilled solution of DMF containing 2 equiv of sodium hydride, followed by addition

dx.doi.org/10.1021/jo200482d |J. Org. Chem. 2011, 76, 5614–5627

Scheme 2. Chemical Derivatization for ^{19}F NMR Analysis

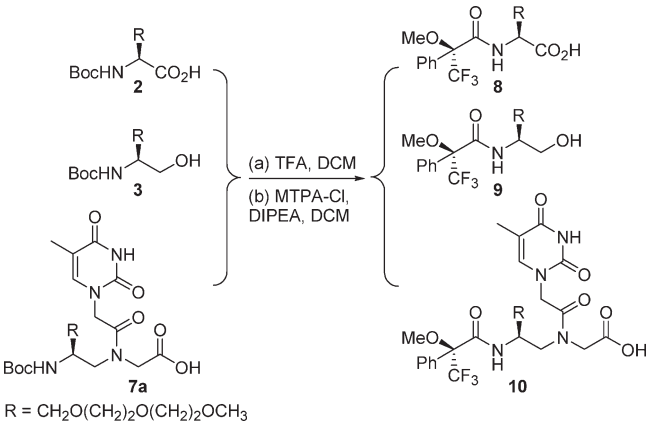

of 1-bromo-2-(2-methoxyethoxy)ethane afforded compound **2** with high optical purity (see the section below). The stoichiometry and order of addition were determined to be essential for obtaining optically pure product. Slow addition of sodium hydride was necessary to ensure complete deprotonation of the carboxyl group prior to removal of the hydroxyl proton. Formation of the carboxylate anion reduces the acidity of the α-proton, making it less susceptible to deprotonation by base. Esterification of the alkylated product **2** followed by reduction with sodium borohydride yielded serinol **3**. This chemical transformation, conversion of the carboxylic acid to alcohol, renders the α-proton inert to deprotonation and racemization in the subsequent reaction steps. Coupling **3** to *N*-[(2,4-dinitrophenyl)sulfonyl]glycine ethyl acetate, which was prepared according to the published procedure,[82] employing the Mitsunobu reaction followed by removal of the (2,4-dinitrophenyl)sulfonyl group with a mild base yielded compound **5**. DCC-mediated coupling of **5** with the appropriate carboxymethylene nucleobases (A,[83] C,[14] G,[83] T[13]) and hydrolysis of the resulting esters gave the desired monomers **7a**−**d**.

Determination of Optical Purities. The optical purities of key intermediates and final monomers were determined by ^{19}F NMR following chemical derivatization (Scheme 2). Corradini and co-workers[84] have previously shown that the enantiomeric excess (ee) of chiral α-PNA monomers and oligomers, with the latter obtained following acid hydrolysis, can be determined by GC/MS following chemical derivatization. We have discovered that ^{19}F NMR is a convenient and accurate alternative method for determining the ee values for γPNA monomers and prior intermediates following removal of the Boc protecting group and subsequent coupling with Mosher's reagent, (+)-1-methoxy-1-(trifluoromethyl)phenylacetyl chloride (MTPA-Cl). Figure 1 shows representative spectra of MTPA-derivatized MP-L-serine **2** (compound **8**), MP-L-serinol **3** (compound **9**), and thymine $^{R\text{-MP}}$γPNA monomer **7a** (compound **10**). The corresponding diastereomers were prepared the same way starting from Boc-D-serine and are included for comparison. A close inspection of these spectra reveals no trace quantity of the other diastereomers for the alkylated serine **8**, serinol **9**, or final monomer **7a**, indicating that they were optically pure. If racemization were to occur, we would expect an additional peak in the spectrum, as indicated by the arrow, corresponding to the chemical shift of the other diastereomer. The ee values for serine **8**, serinol **9**, and final thymine monomer **7a** were estimated to be at least 99%, within the detection limit of ^{19}F NMR.[85] At this point it is not clear why

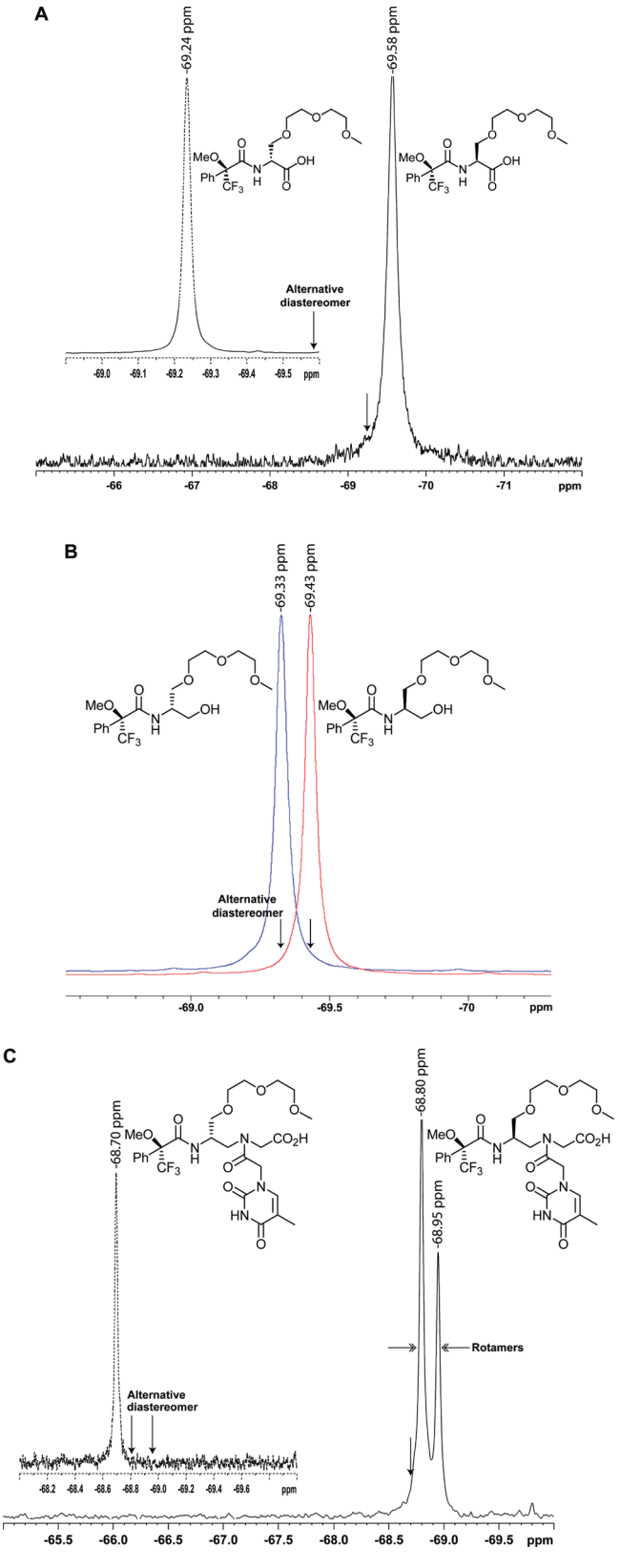

Figure 1. ^{19}F NMR spectra of MTPA-derived (A) MP-L-serine **2** (compound **8**), (B) MP-L-serinol **3** (compound **9**), and (C) thymine monomer **7a** (compound **10**). The corresponding diastereomers were prepared under identical conditions starting from Boc-D-serine and are included for comparison.

dx.doi.org/10.1021/jo200482d |*J. Org. Chem.* 2011, 76, 5614–5627

Table 1. Sequence of PNA Oligomers[a]

oligomer	sequence	no. of MP units
PNA1	H-GCATGTTTGA-NH_2	0
PNA2	H-GCATGTTTGA-NH_2	1
PNA3	H-GCATGTTTGA-NH_2	3
PNA4	H-GCATGTTTGA-NH_2	5
PNA5	H-GCATGTTTGA-NH_2	10
PNA6	H-ACGGGTAGAATAACAT-NH_2	0
PNA7	H-ACGGGTAGAATAACAT-NH_2	1
PNA8	H-ACGGGTAGAATAACAT-NH_2	3
PNA9	H-ACGGGTAGAATAACAT-NH_2	5
PNA10	H-ACGGGTAGAATAACAT-NH_2	8
PNA1X	H-^{L}Orn(X)-^{L}Lys-GCATGTTTGA-NH_2	0
PNA1Y	H-^{L}Lys-GCATGTTTGA-^{L}Orn(Y)-NH_2	0
PNA4X	H-^{L}Orn(X)-^{L}Lys-GCATGTTTGA-NH_2	5
PNA4Y	H-^{L}Lys-GCATGTTTGA-^{L}Orn(Y)-NH_2	5

[a] Underlined letters indicate *R*-MP γ-backbone modification. X = fluorescein (FITC), and Y = tetramethylrhodamine (TAMRA).

the thymine $^{R\text{-MP}}\gamma$PNA monomer showed two rotamers (Figure 1C), at −68.80 and −68.95 ppm, while thymine $^{S\text{-MP}}\gamma$PNA showed only one (Figure 1C, inset). (The existence of the two rotamers was determined by multinuclear and multidimensional NMR analyses as described in an earlier work;[73] they differ from one another in the rotation around the C7−N4 tertiary amide bond.) We attribute the high optical purities of the intermediates and final monomers (the others not shown) to the optimized, initial alkylation step and the stereoselective conversion of carboxylic acid to alcohol in the second step, on the basis of the procedure reported by Rodriguez and co-workers.[86]

Oligomer Design and Synthesis. Three sets of PNA oligomers were prepared (Table 1). The first set, comprising PNA1−5, was designed to test the effects of MP on the conformation and hybridization properties of PNA. The second set, consisting of PNA6−10, was designed to test the effect of MP on water solubility. The hexadecameric sequence was chosen for this study because it represents a statistical length that would be required to target a unique site within the mammalian genome or transcriptome. The third set, constituting PNA1 and PNA4, each separately linked to fluorescein (FITC) at the N-terminus (PNA1X and PNA4X) and tetramethylrhodamine (TAMRA) at the C-terminus (PNA1Y and PNA4), was designed to test the effect of MP on self-aggregation on the basis of Förster resonance energy transfer (FRET). Inclusion of a lysine residue at the C-terminus was necessary, since prior attempts to synthesize FITC- and TAMRA-containing PNA oligomers without the lysine residue resulted in sticky and poorly water soluble materials that were difficult to purify and characterize.

All PNA oligomers, those with and without MP side chains, were synthesized on a solid support according to the published procedures of Christensen and co-workers .[87] Unlike modifications made at the α-backbone, which require further optimization of the reaction condition to minimize racemization during the on-resin coupling,[88] no precaution was necessary for coupling of $^{R\text{-MP}}\gamma$PNA monomers on the resin. Upon completion of the last monomer coupling, the oligomers were cleaved from the resin and precipitated with ethyl ether. After being air-dried, the crude pellets were dissolved in a water/acetonitrile mixture (80:20), purified by reversed-phase HPLC, and characterized by MALDI-TOF mass spectrometry.

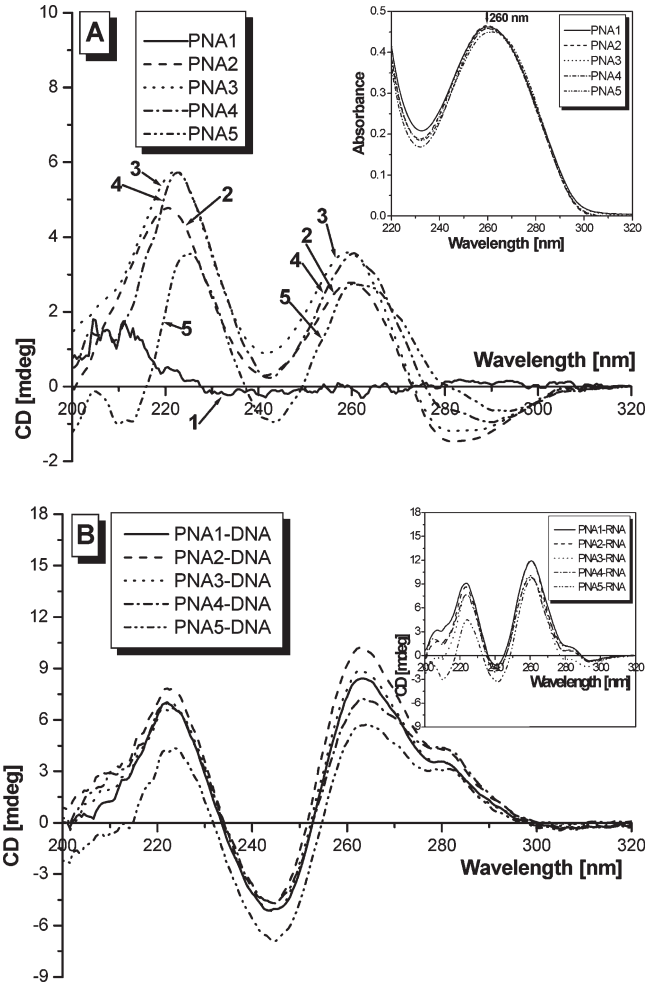

Figure 2. CD spectra of (A) the unhybridized (single-stranded) PNA oligomers and (B) the corresponding PNA−DNA and PNA−RNA (inset) hybrid duplexes at 5 μM strand concentration each. (A) Inset: UV absorption spectra of the individual PNA oligomers at 90 °C, showing that they had the same concentration. This indicates that the differences in the CD spectra, both the amplitude and profile, are the intrinsic properties of the oligomer themselves and not the variations in concentrations. The samples were prepared in 10 mM sodium phosphate buffer at pH 7.4, and the CD spectra were recorded at room temperature. The cDNA strand used was 5′-TCAAACATGC-3′.

Conformational Analysis. To determine the effect of MP on the conformation of PNA, we measured the CD spectra of PNA1−5. Consistent with the earlier finding,[69] we did not observe noticeable CD signals in the nucleobase absorption regions for PNA1 (Figure 2A). This indicates one of two possibilities: either that the PNA does not adopt a helical conformation or that it does but with an equal proportion of a right-handed and left-handed helix. The latter was suggested by MD simulations,[89] but ruled out on the basis of NMR analyses.[69] However, in the case of PNA2−5, we noticed distinct exciton coupling patterns, with minima at 242 and 280 nm and maxima at 220 and 260 nm, characteristic of a right-handed helix.[90] The amplitude of the CD signals remained fairly constant as more MP units were added, but the profiles slightly shifted toward that of the PNA−DNA^2 and PNA−RNA^2 double helices (Figure 2B), especially at the 242 and 280 nm minima. A gradual dip at the 242 nm minimum generally indicates a tightening in the helical pitch of the

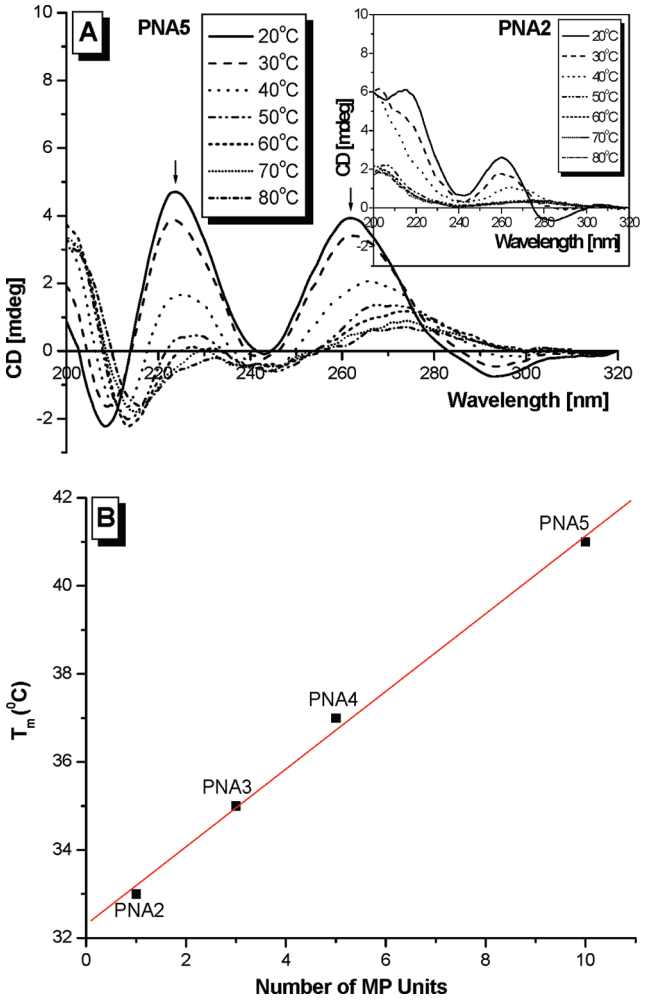

Figure 3. (A) CD spectra of PNA5 and PNA2 (inset) as a function of temperature. (B) Melting transition (T_m) of PNA2−5 as determined by CD, monitored at 260 nm. The oligomer concentration was 5 μM, prepared in 10 mM sodium phosphate buffer at pH 7.4.

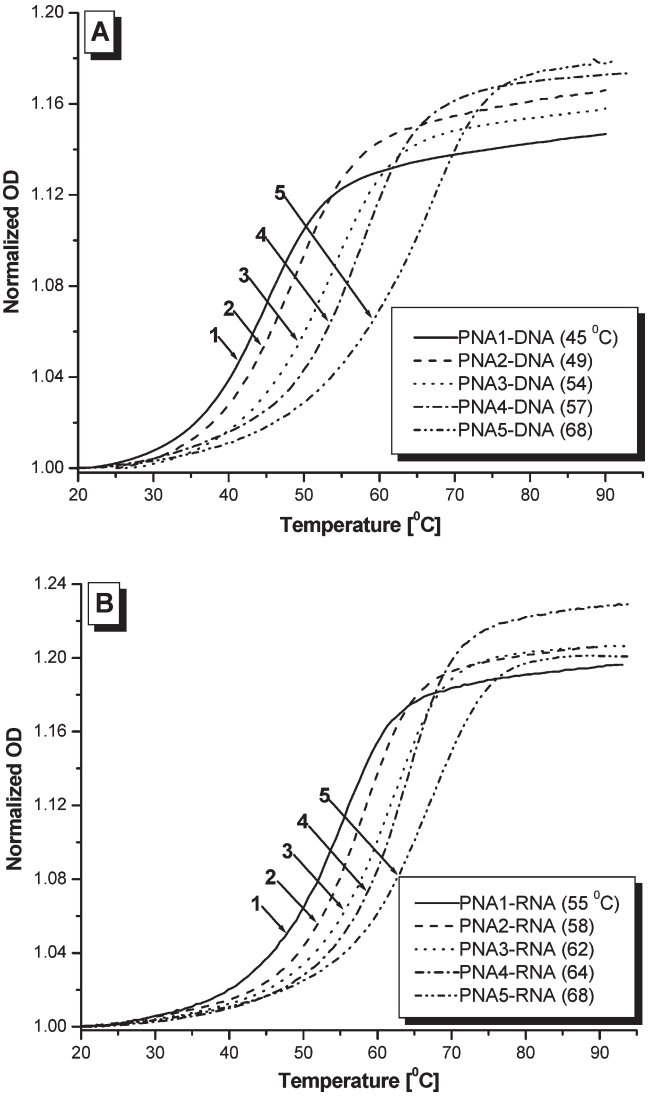

Figure 4. UV melting profiles of (A) PNA−DNA and (B) PNA−RNA hybrid duplexes at 5 μM strand concentration each in 10 mM sodium phosphate buffer at pH 7.4. Both the heating and cooling runs were performed; they both had nearly identical profiles (only the heating runs are shown).

oligomer,[91] from one that resembles that of a PNA−PNA[92] duplex with 18 base pairs per turn to one that resembles that of a PNA−DNA[93] duplex with 13 base pairs per turn. Overall, the CD profiles of PNA2−5 are similar to those of the corresponding PNA−DNA and PNA−RNA hybrid duplexes (Figure 2B). The major difference however is in the amplitude, which is roughly doubled for the duplex as compared to the individual strand. This is because the concentration of bases in the hybrid duplex is twice that of the individual PNA strand. Taken together, these results show that a single (*R*)-MP unit installed at the γ-backbone is sufficient to preorganize PNA into a right-handed helix. Incorporation of additional MP units did not further improve base-stacking, apparent from the similarities in the CD amplitudes, but it did help to tighten the helical pitch of the oligomers, making them more rigid and compact. This is apparent from the temperature-dependent CD measurements, which showed less dramatic reduction in the signal amplitude with temperature for PNA5 as compared to that of PNA2 (Figure 3A). Even at a temperature as high as 80 °C, a distinct CD profile still remained, indicating that base-stacking still occurred at this temperature—whereas it was completely denatured in the case of PNA2. Overall the stability of the oligomers increases linearly with the number of MP units incorporated (Figure 3B). The fact that PNA5 adopts a helical conformation most closely resembling that of PNA−DNA and PNA−RNA duplexes suggests that it would hybridize to DNA and RNA more effectively than the other oligomers in this series.

Thermal Stability. UV melting experiments were performed to determine the effect of MP on the thermal stability of PNA upon hybridization to DNA and RNA. Our result shows that incorporation of a single MP side chain stabilized a PNA−DNA duplex by 4 °C (Figure 4A). The extent of stabilization gradually increased with additional MP units added but tapered off to ~2.3 °C per unit for the fully modified PNA5. A similar pattern was observed for RNA, but the extent of stabilization was less compared to that of DNA (Figure 4B). The enhancement was only 3 °C for the first MP unit incorporated and 1.2 °C per unit for PNA5, as compared to 2.3 °C per unit with DNA. It is interesting to note that the unmodified PNA1 binds more tightly to RNA than to DNA, with a differential T_m (ΔT_m) of 10 °C.

dx.doi.org/10.1021/jo200482d |*J. Org. Chem.* 2011, 76, 5614–5627

Table 2. Thermodynamic Parameters for PNA−DNA and PNA−RNA Duplexes

	PNA−DNA[a]				PNA−RNA[b]			
oligomer	$-\Delta H°$ (kJ/mol)	$-T\Delta S°$ (kJ/mol)	$-\Delta G°$ (kJ/mol)	K_d	$-\Delta H°$ (kJ/mol)	$-T\Delta S°$ (kJ/mol)	$-\Delta G°$ (kJ/mol)	K_d
PNA1	273 ± 5	224 ± 5	49 ± 1[c]	2.5×10^{-9}	289	229	60	3.5×10^{-11}
PNA2	319 ± 18	263 ± 16	54 ± 1	3.2×10^{-10}	333	232	68	1.2×10^{-12}
PNA3	316 ± 11	256 ± 11	59 ± 1[c]	5.1×10^{-11}	350	280	71	4.3×10^{-13}
PNA4	329 ± 14	265 ± 12	65 ± 1	3.5×10^{-12}	356	283	73	1.7×10^{-13}
PNA5	372 ± 11	294 ± 10	78 ± 2	4.6×10^{-14}	365	287	78	2.1×10^{-14}

[a] The averages of three trials (two from concentration dependence measurements and one from UV melting curve fitting). [b] UV melting curve fitting. [c] The standard deviation is less than 1 kJ/mol. The temperature was 298 K.

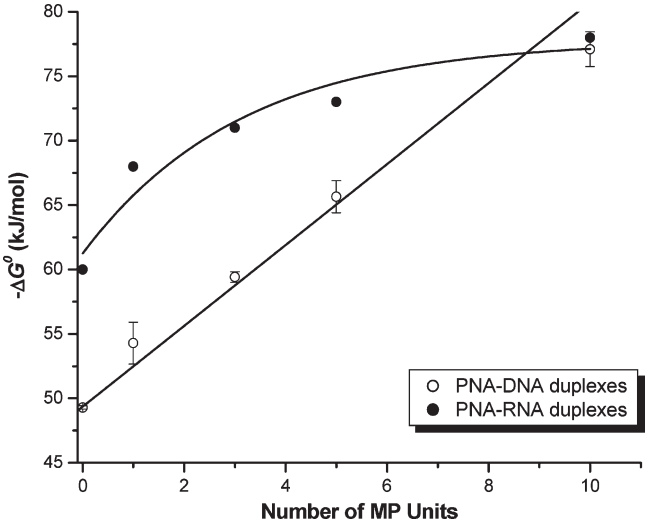

Figure 5. Correlation between the Gibbs binding free energy ($\Delta G°$) and number of MP units.

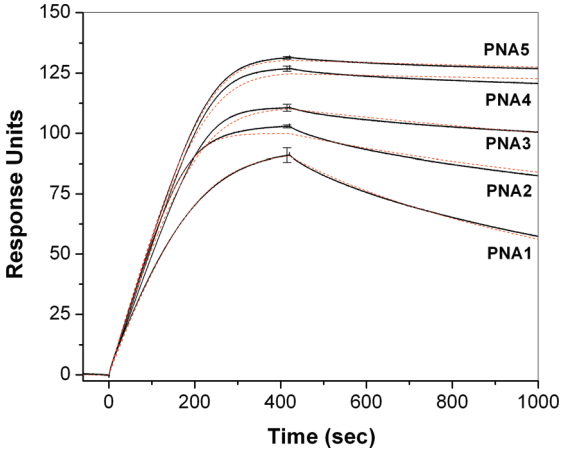

Figure 6. SPR sensorgrams (solid black lines) and fits (red dotted lines) for hybridization of PNA probes to immobilized cDNA. Solutions contained 30 nM PNA. (Sensorgrams and kinetic fits for all PNA concentrations from 10 to 50 nM are provided in the Supporting Information.) Error bars at t = 420 s illustrate standard deviations for three separate trials.

However, fully modified PNA5 displayed thermal stability identical with that of RNA as well as that of DNA. The lack of a preferential binding for PNA5 is not clearly understood at this point, but it may reflect the rigidity of the backbone. Because PNA5 is more rigid and tightly wound as compared to PNA1, it may not have the flexibility or conformational freedom to accommodate the DNA and RNA template strands. Under such circumstances, the DNA and RNA strands would have to undergo a conformational change of their own to accommodate the $^{R\text{-MP}}\gamma$PNA helix and for hybridization to take place. This may explain why $^{S\text{-Ala}}\gamma$PNA−DNA prefers a P-form helix,[73] a structure that is intermediate between the A- and B-form DNA, an indication that DNA and RNA accommodate the γPNA exigencies rather than the other way around. The RNA strand is less accommodating to the $^{R\text{-MP}}\gamma$PNA, when it is fully modified, because the RNA backbone is more rigid as compared to that of DNA due to the presence of the chiral OH group at the 2′-position.[94]

Thermodynamic Analysis. To gain greater insight into the contribution of MP to the stability of the PNA−DNA duplex, we used van't Hoff analysis to determine the thermodynamic parameters for PNA1−5 upon hybridization to cDNA and RNA strands.[95] The data are tabulated in Table 2. Our results show that the Gibbs binding free energy ($\Delta G°$) increases (to a rough approximation) linearly with the number of MP units for PNA−DNA and follows a sigmoidal growth for PNA−RNA (Figure 5). Incorporation of a single MP unit resulted in a net gain in binding free energy of ∼5 kJ/mol for PNA−DNA, whereas it is less for PNA−RNA—especially at the higher end. A reduction in the equilibrium dissociation constant (K_d) by nearly 5 orders of magnitude for PNA5−DNA and 3 orders of magnitude for PNA5−RNA was observed, as compared to that of the respective PNA1−NA and PNA1−RNA duplexes. The binding free energy gain in this case appears to be predominantly enthalpically driven for both PNA−DNA and PNA−RNA, apparent from the gradual increase in the $\Delta H°$ term with the number of MP units concomitant with modest enthalpy−entropy compensation.[96]

Kinetics of Hybridization and Dissociation. From a kinetic perspective, the higher apparent affinity of the $^{R\text{-MP}}\gamma$PNA oligomers indicated by the UV melting curves, from which the equilibrium dissociation constants were extracted, could be due to faster on rates and/or slower off rates. We used surface plasmon resonance (SPR) analysis to study the hybridization kinetics. In most other examples of PNA−DNA hybridization studied by SPR, the PNA probe was immobilized to the chip while the DNA target was captured from solution.[97−99] One exception was previous work from our group, in which a DNA guanine quadruplex target was immobilized and a homologous PNA probe hybridized to form a PNA−DNA heteroquadruplex.[100,101] In the current studies, a biotinylated version of the DNA target was immobilized on a streptavidin-conjugated, carboxymethylated

dx.doi.org/10.1021/jo200482d |J. Org. Chem. 2011, 76, 5614–5627

Table 3. Association Rate Constant (k_a), Dissociation Rate Constant (k_d), and Equilibrium Dissociation Constant (K_d) for Hybridization of PNA Probes with a Complementary DNA Target

oligomer	k_a ($M^{-1}s^{-1}$)	k_d (s^{-1})	K_d (M)
PNA1	4.7×10^5	13.0×10^{-4}	2.8×10^{-9}
PNA2	9.7×10^5	4.1×10^{-4}	4.2×10^{-10}
PNA3	6.2×10^5	1.9×10^{-4}	3.0×10^{-10}
PNA4	6.6×10^5	0.3×10^{-4} [a]	4.1×10^{-11} [a]
PNA5	8.0×10^5	0.4×10^{-4} [a]	5.4×10^{-11} [a]

[a] Uncertainty due to the calculated value approaching the limits of detection of the instrument.

dextran chip. A relatively low surface density (ca. 100 response units) of DNA target was used to limit mass transport effects on the association kinetics. Solutions containing 10−50 nM PNA were allowed to flow over the chip for 420 s, at which point the flow was switched to a PNA-free buffer to allow net dissociation of the hybridized PNA.

Individual sensorgrams for the unmodified (PNA1) and $^{R\text{-MP}}\gamma$-modified (PNA2−5) oligomers at 30 nM concentration are shown in Figure 6. Relatively minor variation is observed in the association kinetics, although singly modified PNA2 appears to bind approximately twice as fast as the unmodified PNA. Fitting the data to a 1:1 binding model yields association rate constants (k_a) that range from 4.7×10^5 to 9.7×10^5 M^{-1} s^{-1} (Table 3). In contrast, significantly larger effects are seen in the dissociation phase of the experiment, with the dissociation rate constant (k_d) varying by at least a factor of 50. Equilibrium dissociation constants (K_d) calculated from the ratio of the dissociation and association rate constants are also given in Table 3. Unmodified PNA1 and fully modified PNA5 have K_d = 2.8 nM and 54 pM, respectively. Note that the K_d values for PNA1−3 determined by SPR (Table 3) are similar to those determined by UV melting experiments (Table 2). However, increasing divergences are observed for PNA4 and PNA5, with the SPR-derived values being 12- and 1200-fold greater, respectively. We attribute this discrepancy to the very small degrees of dissociation observed within the time scale of the SPR experiment. This introduces a large uncertainty into the fitting of the dissociation phases of the sensorgrams, translating into questionable K_d values. However, we also note that the free energy changes given in Table 2 are based on the assumption that the heat capacity change for PNA−DNA melting is zero, allowing the parameters determined at the high melting temperature to be extrapolated to lower temperatures. Future calorimetric measurements will allow us to determine whether there is a heat capacity change in these hybridization/melting transitions. Nevertheless, the SPR results clearly demonstrate that the enhanced affinity of the $^{R\text{-MP}}\gamma$PNAs is due almost entirely to the significantly slower dissociation kinetics. Thus, the helical preorganization of the modified PNA does not translate into significantly faster hybridization. This could be due to the fact that the cDNA strand is likely to require some structural reorganization of its own to hybridize to the PNA, negating the preorganization of the latter. While the origin of the slower dissociation kinetics is not clear at this time, one possible contributor is the network of structured water molecules in the minor groove of the hybrid duplex, which would need to be disrupted to separate the two strands.

Sequence Selectivity. On the basis of the CD, NMR,[69] and X-ray[73] data which showed that γPNAs derived from L-amino acids adopt a right-handed helix and that the helix becomes more rigid as more γ-chiral units are added in the backbone, one would expect a fully modified PNA5 to hybridize to DNA and RNA targets with greater sequence selectivity than PNA1. To verify this prediction, we determined the thermal stabilities of PNA5−DNA and PNA5−RNA duplexes containing perfectly matched (PM) and single-base-mismatched (MM) targets and compared them to those from an earlier study with PNA1−DNA and PNA1−RNA.[69] Our results showed that, despite the strong binding affinity, PNA5 is able to discriminate between closely related sequences. ΔT_m ranges from −17 to −21 °C for PNA5−DNA and from −16 to −20 °C for PNA5−RNA containing a single-base mismatch (X = C, G, T), as compared to −10 to −14 °C for PNA1−DNA and −11 to −18 for PNA1−RNA (Table 4). The level of sequence discrimination is greater for PNA5−DNA than for PNA1−DNA, and similar, if not slightly better, for PNA5−RNA as compared to PNA1−RNA. This result is consistent with PNA5 adopting a more rigid helical motif, which is less accommodating to structural mismatches as compared to PNA1.

Table 4. Sequence Mismatch Discrimination[a]

	T_m (°C)		T_m (°C)	
X−T	PNA1−DNA[b]	PNA5−DNA	PNA1−RNA[b]	PNA5−RNA
A−T	45	68	55	68
C<>T	31 (−14)[c]	47 (−21)	37 (−18)	48 (−20)
G<>T	31 (−14)	48 (−20)	44 (−11)	52 (−16)
T(U)<>T	35 (−10)	51 (−17)	40 (−15)	48 (−20)

[a] Sequences: PNA1, H-GCATGTTTGA-^{L}Lys-NH_2; PNA5, H-GCA-TGTTTGA-^{L}Lys-NH_2; DNA, 3′-CGTACAXACT-5, X = A, C, G, T; RNA, 3′-CGUACAXACU-5, X = A, C, G, U. [b] The data for PNA1−DNA and PNA1−RNA mismatched binding were taken from ref 69. [c] The value in parentheses indicates ΔT_m between the perfect match and mismatch.

Table 5. Saturated Concentrations of PNA Oligomers

oligomer	no. of MP units	satd concn (mM)
PNA6	0	39
PNA7	1	76
PNA8	3	108
PNA9	5	350
PNA10	8	>500

Water Solubility. To determine whether inclusion of MP in the backbone has an effect on water solubility, we determined the saturating concentrations of PNA6−10 (Table 1) in aqueous solution using UV spectroscopy. It is interesting to note that incorporation of a single MP unit enhanced the solubility of PNA6 by nearly 2-fold (Table 5). The solubility of the oligomers is further improved, albeit to a smaller extent, with additional MP units. For PNA8, which contained eight MP units, we could not determine the saturating concentration of this oligomer because addition of a minimum amount of water (1 μL) into a vial containing 2.7 mg of fluffy material resulted in complete dissolution. On the basis of this result, we estimated the saturating concentration to be at least 500 mM—more than an order of magnitude higher than that of the unmodified PNA6. Solvation of the MP side chain likely contributes to the enhanced solubility. The other contributing factor may come from helical organization. Stacking the nucleobases on top of one another in a helical arrangement

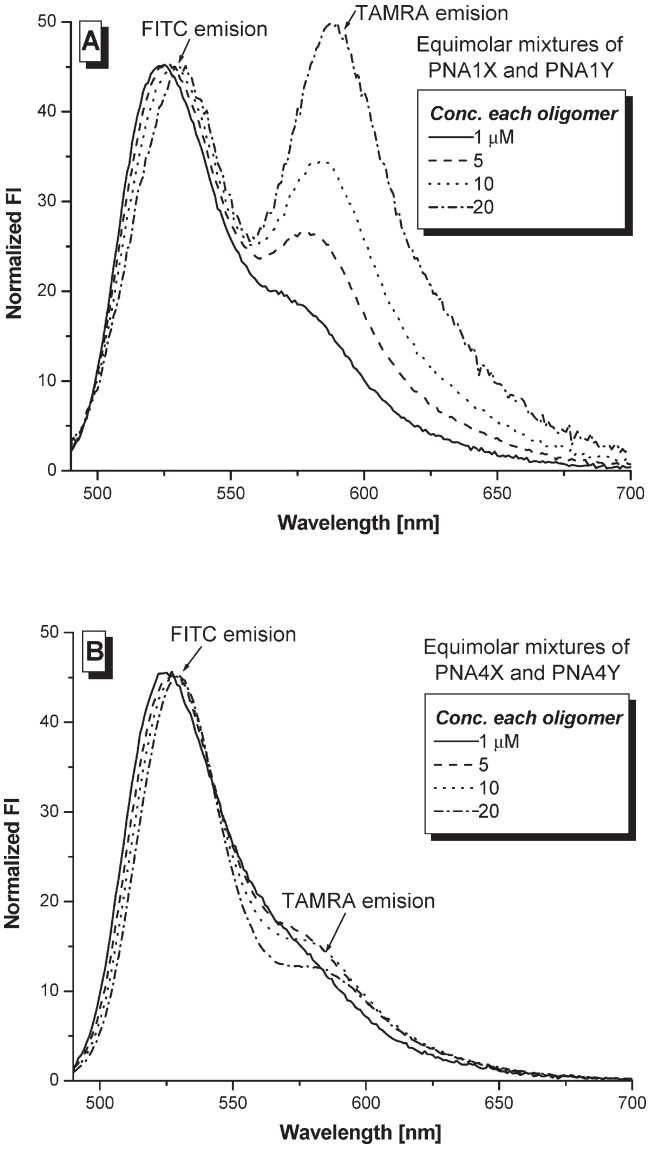

Figure 7. Fluorescent spectra of (A) PNA1X−PNA1Y and (B) PNA4X−PNA4Y pairs at different concentrations. The samples were prepared by mixing equimolar ratios of the oligomers in 10 mM sodium phosphate buffer (pH 7.4). The samples were excited at 475 nm (FITC λ_{max}), and the emissions were recorded from 480 to 700 nm. The spectra were normalized with respect to the FITC emission.

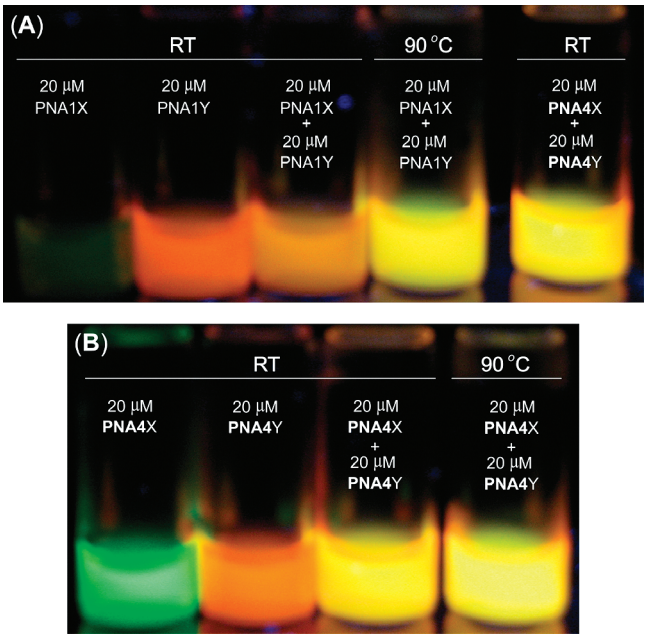

Figure 8. Photographs of (A) PNA1X−PNA1Y and (B) PNA4X−PNA4Y samples at different temperatures upon excitation with a short-wavelength (254 nm), hand-held UV lamp. The sample indicated as "90 °C" was incubated in a heating block at 90 °C for 5 min prior to placement on the UV lamp, after which the photographs were immediately taken.

would shield the hydrophobic core from exposure to solvent. As such, only the heteroatoms at the periphery of nucleobases are exposed to and interact with the water molecules. This may explain the nonlinear relationship between the number of MP units and the saturating concentrations of PNA oligomers.

This suggestion was corroborated by additional experiments (Figure S1, Supporting Information) which showed that incorporation of a single methyl group instead of MP at the γ-backbone of PNA resulted in nearly 1.2-fold improvement in water solubility, while the reversed trend was observed with additional methyl groups. This is because addition of the alkyl group beyond the first unit does not help to preorganize PNA any more than it already has but instead introduces additional hydrophobic character to the backbone. This would exacerbate self-aggregation, leading to formation of large molecular weight complexes and precipitation of the aggregates out of the solution.

Self-Aggregation. Next we performed a FRET study to determine whether incorporation of MP into the backbone of PNA would also help reduce aggregation. Different concentrations of unmodified PNA1X−PNA1Y and homologous γ-modified PNA4X−PNA4Y pairs (Table 1) were prepared by mixing equimolar ratios of the individual oligomers in sodium phosphate buffer. The samples were excited at 475 nm, the λ_{max} of FITC, and the emission was recorded from 480 to 700 nm. Upon aggregation, in which the oligomers bearing FITC and TAMRA come into contact with one another, excitation at 475 nm would lead to energy transfer from FITC to TAMRA because of the proximity of the two chromophores. Comparison of the FRET efficiencies of the two systems at different concentrations should provide an assessment of the effect of MP on the intermolecular interaction of PNA.

Inspection of Figure 7A reveals that, at a concentration as low as 1 μM of each PNA oligomer, a small but noticeable emission appeared at 580 nm, an indication of FRET and correspondingly aggregation between PNA1X and PNA1Y. The extent of aggregation was further intensified with increasing concentrations of oligomers, apparent from the fluorescent intensity of TAMRA at ~580 nm upon excitation of the FITC donor at 475 nm. In contrast, at 20 μM, the point at which nearly 70% FRET efficiency was observed for PNA1X−PNA1Y, only ca. 5% FRET efficiency was observed for PNA4X−PNA4Y (Figure 7B). This indicates that the pair of γ-modified PNAs do not interact with each other as much as the unmodified PNAs. The distinction is apparent from photographs of the samples illuminated with a short-wavelength (254 nm), hand-held UV lamp (Figure 8). The PNA1X−PNA1Y solution displayed a light orange emission at

dx.doi.org/10.1021/jo200482d |J. Org. Chem. 2011, 76, 5614–5627

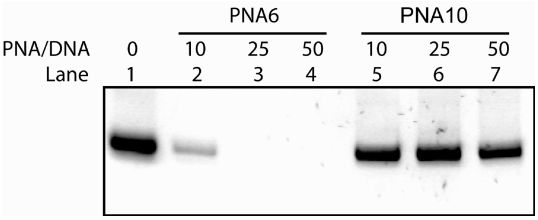

Figure 9. Result of a gel-shift assay following incubation of a 171 bp, linear double-stranded DNA with different concentrations of PNA6 and PNA10 in 10 mM sodium phosphate buffer (pH 7.4) at 37 °C for 16 h, followed by electrophoretic separation on nondenaturing gel and SYBR-Gold staining. Note that this particular DNA fragment, which was PCR amplified from a Psuper plasmid vector, does not have a sequence complementary to that of PNA6 or PNA10 (both contained the same nucleobase sequence). The concentration of the 171 bp DNA fragment was 0.4 μM.

room temperature and yellow-green hue at 90 °C, an indication of the aggregate dissociating upon heating. In contrast, the PNA4X—PNA4Y solution displayed the same color, yellow-green, at room temperature as well at 90 °C, indicating that the oligomers were well dispersed even at room temperature. Thus, the *R*-MP γ-modification not only imparts enhanced solubility to PNA, but also suppresses aggregation.

Off-Target Binding. It has been documented that, at moderate concentrations, PNA tends to aggregate and stick to surfaces and other macromolecules in a nonspecific manner.[33] Such interactions could lead to off-target binding and cytotoxic effects when employed in the cellular context. Among the macromolecules that PNA is known to interact nonspecifically with are nucleic acids and proteins.[34] To assess the extent of off-target binding of PNA and $^{R\text{-MP}}\gamma$PNA, we performed a gel-shift assay. In this case a DNA fragment (PCR product), 171 bp in length, was incubated with different concentrations of PNA6 and PNA10 (Table 1) in 10 mM sodium phosphate buffer at 37 °C for 16 h. The two oligomers contained identical nucleobase sequences but differed from another at the γ-backbone; PNA6 was unmodified, whereas PNA10 was modified at every other position with an *R*-MP γ side chain. Following incubation, the samples were separated on nondenaturing polyacrylamide gel and stained with SYBR-Gold.

Since the target did not contain a sequence complementary to that of the oligomers, we did not expect binding to take place, in which case the intensity of the DNA band should remain fairly constant, independent of the PNA6 and PNA10 concentrations. Instead, we observed a drastic reduction in the intensity of the DNA band with increasing concentrations of PNA6 (Figure 9). At 10 μM (corresponding to a PNA:DNA ratio of 25:1) or higher, the DNA band completely disappeared from the gel. We observed neither a shifted band, indicating formation of a stable complex, nor staining in the wells, which would indicate formation of globular complexes too large to traverse through the polyacrylamide gel. One possible explanation for the disappearance of the DNA band could be that, once formed, the PNA—DNA complex precipitated from solution and/or adhered to the walls of the eppendorf tubes in which the samples were incubated. On the other hand, for γ-modified PNA10, the intensity of the DNA bands remained fairly constant even at a concentration as high as 20 μM (PNA:DNA ratio of 50:1). This result is consistent with the solubility and FRET data, indicating that incorporation of MP at the γ-backbone not only improves the hybridization properties and water solubility of PNA but also helps reduce nonspecific binding with other macromolecules as well—in this case DNA.

CONCLUSION

In summary, we have shown that a randomly folded PNA can be preorganized into a right-handed helix by installing an *R*-MP side chain at the γ-backbone. The MP-containing γPNA monomers can be prepared in a few simple steps starting from a commercially available and relatively cheap Boc-L-serine. We attribute the high optical purities of the backbone intermediates and final monomers to the optimized alkylation condition in the first step and stereoselectivity of the reduction of carboxylic acid to alcohol in the second step. In contrast to the (aminoethyl)-glycine backbone prepared via the reductive amination route, which degrades over time (unpublished data), compound **4** can be stored over a prolonged period without signs of deterioration. Another appealing feature of γ-backbone modification is that it is configurationally stable. After the reduction step, i.e., conversion of the carboxylic acid to alcohol, the γ-proton is inert to deprotonation by base. Thus, there is no need for concern for racemization in the subsequent reaction steps. Compared to the previous attempts to improve water solubility, which is often achieved at the expense of binding affinity and/or sequence selectivity, incorporation of MP in the γ-backbone enhances the hybridization properties as well as the water solubility of PNA. Improvements in thermodynamics are attributed to slower dissociation, while enhanced sequence selectivity is the result of backbone preorganization and helical base-stacking arrangement. Improvement in water solubility is the result of solvation of the MP side chains as well as helical nucleobase arrangement. Helical induction presumably permits greater shielding of the hydrophobic cores of nucleobases and better hydrogen-bonding interaction between heteroatoms at the periphery of nucleobases and solvent molecules.

The results reported herein have important implications for the future design and utility of PNA in biology, biotechnology, and medicine. The improvements in hybridization properties may enable $^{R\text{-MP}}\gamma$PNAs to invade double-helical DNA and structured RNA, which may not be permissible with other classes of oligonucleotide mimics. The former has already been demonstrated in a recent study.[81] The enhancements in water solubility will facilitate the handling and processing of PNA while lessening the concerns for nonspecific binding and cytotoxic effects. Improvements in these areas, along with the flexibility of synthesis whereby other chemical functionalities can be installed at the γ-backbone with ease, will further expand the utility of PNA into other burgeoning disciplines, including drug discovery and nanotechnology.

EXPERIMENTAL SECTION

Monomer Synthesis. *Boc-(2-(2-methoxyethoxy)ethyl)-L-serine (**2**).* To a stirred, ice-cold (0 °C) solution of NaH (60% suspended in mineral oil, 1.7 g, 42.6 mmol) in dry DMF (80 mL) under an inert atmosphere was added Boc-L-Ser-OH (4.05 g, 19.6 mmol) in DMF (30 mL) dropwise over a period of 3 h. To this mixture, while still in the ice bath, was added 1-bromo-2-(2-methoxyethoxy)ethane (6.4 mL, 42.6 mmol) at once. The ice bath was then removed, and the reaction was allowed to gradually warm to room temperature and stirred for another 3 h. The reaction mixture was quenched with H_2O (100 mL) at 0 ^{o}C. The solvents (DMF and water) were evaporated under reduced pressure at room temperature. Water (20 mL) was added to the crude

residue and acidified with 5% HCl to pH ≈ 3 at 0 °C. The aqueous layers were extracted with ethyl acetate (5 × 100 mL) and dried over Na_2SO_4. The solvent was evaporated under reduced pressure, and the crude mixture was purified by column chromatography to afford a colorless liquid (4.1 g, 13.3 mmol): yield 68%; ^{1}H NMR ($CDCl_3$, 300 MHz) δ 6.84 (br s, 1H), 5.57 (d, J = 7.4 Hz, 1H), 4.46−4.38 (m, 1H), 3.93 (dd, J_1 = 3.9 Hz, J_2 = 3.5 Hz, 1H), 3.90−3.49 (m, 9H), 3.37 (s, 3H), 1.41 (s, 9H); ^{13}C NMR ($CDCl_3$, 75 MHz) δ 28.2, 53.8, 58.7, 70.2, 70.7, 70.9, 71.7, 80.0, 155.8, 173.4; HRMS (ESI/$MS_{m/z}$) M calcd for $C_{13}H_{25}NO_7$Na 330.1529, found 330.1546.

*Boc-(2-(2-methoxyethoxy)ethyl)-L-serinol (**3**).* To a stirred solution of Boc-(2-(2-methoxyethoxy)ethyl)-L-serine (**2**) (4 g, 13.0 mmol) in 20 mL of DME in an ice bath was added NMM (1.43 mL, 13.0 mmol) dropwise under an inert atmosphere, followed by isobutyl chloroformate (1.76 mL, 13.0 mmol). The reaction mixture was stirred at the same temperature for another 0.5 h. The cold solution was filtered, and the precipitate was washed with DME (2 × 10 mL). To the combined filtrate stirred in an ice bath was added $NaBH_4$ (0.741 g, 19.5 mmol in 10 mL water) slowly. *A strong effervescence occurred.* The aqueous layer was extracted three times with ethyl acetate, and the combined organic layers were washed with brine and dried over Na_2SO_4. The solvent was evaporated under reduced pressure, and the oily residue was purified by column chromatography to give a colorless liquid (3.2 g, 10.9 mmol): yield 84%; ^{1}H NMR ($CDCl_3$, 300 MHz) δ 5.26 (br s, 1H), 3.84−3.50 (m, 12 H), 3.36 (s, 3H), 2.93 (br s, 1H), 1.42 (s, 9H); ^{13}C NMR ($CDCl_3$, 75 MHz) δ 28.3, 51.5, 58.9, 63.2, 70.3, 70.4, 70.5, 71.3, 71.8, 79.5, 156.0; HRMS (ESI/$MS_{m/z}$) M calcd for $C_{13}H_{27}NO_6$Na 316.1736, found 316. 1719.

*Boc-(2-(2-methoxyethoxy)ethyl)-L-serine-Ψ[CH_2N(o,p-diNBS)]Gly-OEt (**4**).* To a stirred, cold solution of *o*,*p*-diNBS-Gly-OEt (3.53 g, 10.5 mmol), triphenylphosphine (2.73 g, 10.5 mmol), and compound **3** (3.1 g, 10.5 mmol) in dried THF (20 mL) under an inert atmosphere was added DIAD (1.48 mL, 10.5 mmol) dropwise over a period of 0.5 h. The reaction mixture was allowed to warm to room temperature and then stirred overnight. The solvent was evaporated, and the oily residue was purified by column chromatography to afford a yellow solid (3.6 g, 5.91 mmol): yield 56%; ^{1}H NMR ($CDCl_3$, 300 MHz) δ 8.51 (dd, J = 2.1 Hz, 1H), 8.41 (d, J = 2.1 Hz, 1H), 8.32 (d, J = 8.7 Hz, 1H), 5.16 (d, J = 8.6 Hz, 1H), 4.34 (dd, J = 18.6 Hz, 2H), 4.10 (2 × q, J = 3.6 Hz, 2H), 4.01−3.87 (m, 1H), 3.70−3.49 (m, 12H), 3.39 (s, 3H), 1.43 (s, 9H), 1.23 (t, J = 7.1 Hz, 3H); ^{13}C NMR ($CDCl_3$, 75 MHz) δ 14.0, 28.2, 48.3, 48.7, 49.6, 58.9, 61.6, 70.0, 70.3, 70.4, 70.8, 71.9, 79.7, 119.4, 126.0, 132.0, 138.4, 147.9, 149.5, 155.6, 168.6; HRMS (ESI/$MS_{m/z}$) M calcd for $C_{23}H_{36}N4O_{13}$SNa 631.1898, found 631.1840.

*Boc-(2-(2-methoxyethoxy)ethyl)-L-serine-Ψ[CH_2N]Gly-OEt (**5**).* To a stirred solution of **4** (2.6 g, 4.2 mmol) in dichloromethane (20 mL) was added *n*-propylamine (7.0 mL, 85.4 mmol) under an inert atmosphere. The reaction mixture was stirred at room temperature for another 20 min. The solvent was evaporated, and the crude mixture was purified by column chromatography to afford **5** as a light yellow liquid (1.3 g, 3.4 mmol): yield 81%; ^{1}H NMR ($CDCl_3$, 300 MHz) δ 5.13 (br s, 1H), 4.12 (q, J = 7.0 Hz, 2H), 3.78−3.63 (m, 1H), 3.62−3.33 (m, 12H), 3.32 (s, 3H), 2.71 (2 × dd, J_1 = J_2 = 5.9 Hz, 2H), 1.80 (br s, 1H), 1.39 (s, 9H), 1.22 (t, J = 7.3 Hz, 3H); ^{13}C NMR ($CDCl_3$, 75 MHz) δ 14.2, 28.3, 49.9, 50.3, 51.0, 58.9, 60.5, 70.4, 70.6, 71.4, 71.9, 79.1, 155.6, 172.4; HRMS (ESI/$MS_{m/z}$) M calcd for $C_{17}H_{34}N_2O_7$Na 401.2264, found 401.2278.

*Boc-(2-(2-methoxyethoxy)ethyl)-L-serine Thymine Ethyl Ester (**6a**).* To a stirred solution of thymine acetic acid (0.287 g, 1.56 mmol) in dried DMF (15 mL) under an inert atmosphere were added DCC (0.324 g, 1.56 mmol) and DhbtOH (0.254 g, 1.56 mmol). The resulting mixture was stirred at room temperature for 1 h. Compound **5** (0.5 g, 1.32 mmol) was dissolved in dried DMF (10 mL) and added to the above reaction mixture, and the resulting mixture was stirred at 50 °C for 24 h. The solvent was removed under reduced pressure, and the remaining residue was dissolved in ethyl acetate (100 mL) and washed with a saturated solution of $NaHCO_3$ (100 mL) followed by 10% $KHSO_4$ (100 mL). The organic layer was washed with brine (50 mL) and dried over Na_2SO_4. The solvent was removed under reduced pressure. The crude product was purified by column chromatography to afford a white solid (0.480 g, 0.88 mmol): yield 67%; ^{1}H NMR (DMSO-d_6, 300 MHz) δ 7.27−7.19 [2 × d ($Rot_{1,2}$), J_1 = J_2 = 1.0 Hz, 1H], 6.86−6.57 [2 × d ($Rot_{1,2}$) [two rotamers were found, as determined by multinuclear and multidimensional NMR experiments[73]], J_1 = J_2 = 8.6 Hz, 1H], 4.80−4.36 [2 × ABq ($Rot_{1,2}$), J_1 = J_2 = 16.8 Hz, 2H], 4.33−3.65 (m, 5H), 3.58−3.25 (m, 12H), 3.22−3.15 [2 × s($Rot_{1,2}$), 3H], 1.73 (s, 3H), 1.35 (br s, 9H), 1.27−1.11 [2 × t($Rot_{1,2}$), J_1 = J_2 = 7.1 Hz, 3H]; ^{13}C $NMR_{major\ rotamer}$ (DMSO-d_6, 75 MHz) δ 12.3, 14.4, 28.6, 47.9, 48.1, 48.6, 49.5, 58.5, 60.9, 70.0, 70.3, 71.7, 78.6, 108.5, 142.4, 151.4, 155.8, 164.8, 168.0, 169.3; HRMS (ESI/$MS_{m/z}$) M calcd for $C_{24}H_{40}N_4O_{10}$Na 567.2642 found, 567.2651.

*Boc-(2-(2-methoxyethoxy)ethyl)-L-serine Adenine(Cbz) Ethyl Ester (**6b**).* Adenine ester **6b** was prepared, purified, and characterized the same way as described for **6a**: ^{1}H NMR (DMSO-d_6, 300 MHz) δ 10.56 (br s, 1H), 8.59−8.55 [2 × s ($Rot_{1,2}$), 1H], 8.30−8.24 [2 × s ($Rot_{1,2}$), 1H], 7.55−7.20 (m, 5H), 7.04−6.53 [2 × d ($Rot_{1,2}$), J_1 = J_2 = 8.5 Hz, 1H], 5.35 [ABq (Rot_1), J = 17.2 Hz, Rot_2 appears as a br s at 5.15 ppm, 2H], 5.20 (s, 2H), 4.54−3.87 (m, 5H), 3.81−3.31 (m, 12H), 3.23−3.10 [2 × s ($Rot_{1,2}$), 3H], 1.36 (s, 9H), 1.30−1.10 [2 × t ($Rot_{1,2}$), J_1 = J_2 = 7.1 Hz, 3H]; ^{13}C $NMR_{major\ rotamer}$ (DMSO-d_6, 75 MHz) δ 14.4, 28.6, 44.3, 48.7, 49.3, 49.9, 58.4, 60.9, 66.7, 70.0, 70.2, 70.4, 71.0, 71.6, 78.7, 123.4, 128.3, 128.4, 128.8, 136.8, 145.5, 149.9, 151.9, 152.7, 152.9, 155.8, 167.4, 169.2; HRMS (ESI/$MS_{m/z}$) M calcd for $C_{32}H_{45}N_7O_{10}$Na 710.3126, found 710.3110.

*Boc-(2-(2-methoxyethoxy)ethyl)-L-serine PNA Guanine(Cbz) Ethyl Ester (**6c**).* Guanine ester **6c** was prepared, purified, and characterized the same way as described for **6a**: ^{1}H NMR (DMSO-d_6, 300 MHz) δ 7.78−7.74 [2 × s ($Rot_{1,2}$), 1H], 7.45−7.28 (m, 5H), 6.98−6.59 [2 × d ($Rot_{1,2}$), J_1 = J_2 = 8.5 Hz, 1H], 5.23 (s, 2H), 5.20−4.84 [ABq (Rot_1), J = 17.1 Hz, m (Rot_2), 2H], 4.45−3.77 (m, 5H), 3.76−3.33 (m, 12H), 3.22−3.11[2 × s ($Rot_{1,2}$), 3H], 1.38−1.28 [2 × s ($Rot_{1,2}$), 9H], 1.28−1.10 [2 × t ($Rot_{1,2}$), J_1 = J_2= 7.2 Hz, 3H]; ^{13}C $NMR_{major\ rotamer}$ (DMSO-d_6, 75 MHz) δ 14.4, 28.5, 44.1, 48.8, 49.4, 49.8, 58.4, 61.0, 67.7, 70.0, 70.1, 70.2, 70.4, 71.6, 78.4, 119.6, 128.5, 128.6, 128.8, 128.9, 135.9, 140.8, 147.8, 149.9, 155.0, 155.6, 155.8, 167.4, 169.2; HRMS (ESI/$MS_{m/z}$) M calcd for $C_{32}H_{45}N_7O_{11}$Na 726.3075, found 726.3070.

*Boc-(2-(2-methoxyethoxy)ethyl)-L-serine PNA Cytosine(Cbz) Ethyl Ester (**6d**).* Cytosine ester **6d** was prepared, purified, and characterized the same way as described for **6a**: ^{1}H NMR (DMSO-d_6, 300 MHz) δ 7.84 (d, J = 7.3 Hz, 1H), 7.46−7.26 (m, 5H), 6.99 (d, J = 7.3 Hz, 1H), 6.87−6.57 [2 × d ($Rot_{1,2}$), J_1 = J_2 = 8.4 Hz, 1H], 5.17 (s, 2H), 4.93−4.52 [2 × ABq ($Rot_{1,2}$), J_1 = J_2 = 15.9 Hz, 2H], 4.37−3.68 (m, 5H), 3.63−3.29 (m, 12H), 3.22−3.15 [2 × s ($Rot_{1,2}$), 3H], 1.35 (s, 9H), 1.27−1.09 [2 × t ($Rot_{1,2}$), J_1= J_2= 7.1 Hz, 3H]; ^{13}C $NMR_{major\ rotamer}$ (DMSO-d_6, 75 MHz) δ 14.4, 28.6, 48.7, 49.9, 58.5, 60.9, 66.9, 70.0, 70.3, 71.7, 78.6, 94.3, 128.3, 128.6, 128.9, 136.4, 151.1, 153.6, 155.4, 155.7, 163.6, 167.9, 169.2; HRMS (ESI/$MS_{m/z}$) M calcd for $C_{31}H_{45}N_5O_{11}$Na 686.3013, found 686.3006.

*Boc-(2-(2-methoxyethoxy)ethyl)-L-serine Thymine Monomer (**7a**).* To a stirred, cold solution of **6a** (0.480 g, 0.88 mmol) in THF (10 mL) was added 2 N NaOH (10 mL) dropwise over a period of 15 min. The resulting mixture was stirred at the same temperature for another 0.5 h. Upon completion of the reaction, as confirmed by TLC, H_2O (20 mL) was added, and the resulting mixture was extracted with ethyl acetate (2 × 25 mL). The aqueous layers were combined, acidified with 5% HCl to pH ≈ 4 at 0 °C, and then extracted with ethyl acetate (4 × 25 mL) and dried over Na_2SO_4. The solvent was evaporated in vacuo, and the crude product was purified by column chromatography to afford a colorless solid (0.400 g, 4.5 mmol): yield 87%; ^{1}H NMR (DMSO-d_6, 300 MHz) δ

7.27−7.18 [2 × s ($Rot_{1,2}$), 1H], 6.88−6.53 [2 × d ($Rot_{1,2}$), $J_1 = J_2$ = 8.2 Hz, 1H], 4.75−4.33 [ABq (Rot_1), J = 17.5 Hz, m (Rot_2), 2H], 4.01−3.59 (m, 3H), 3.55−3.25 (m, 12H), 3.22−3.19 [2 × s ($Rot_{1,2}$), 3H], 1.73 (s, 3H), 1.35 (s, 9H); ^{13}C $NMR_{major\ rotamer}$ (DMSO-d_6, 75 MHz) δ 12.3, 28.7, 48.1, 49.3, 51.9, 58.5, 70.0, 70.2, 70.3, 71.0, 71.7, 78.2, 78.5, 108.5, 142.6, 151.5, 155.7, 164.8, 167.5, 168.5; HRMS (ESI/$MS_{m/z}$) M calcd for $C_{22}H_{35}N_4O_{10}Na_2$ 561.2148, found 561.2115.

*Data for Boc-(2-(2-methoxyethoxy)ethyl)-L-serine adenine(Cbz) monomer (**7b**):* ^{1}H NMR (DMSO-d_6, 300 MHz) δ 8.57−8.53 [2 × ($Rot_{1,2}$), 1H], 8.30−8.16 [2 × s ($Rot_{1,2}$), 1H], 7.47−7.24 (m, 5H), 7.04−6.50 [2 × d ($Rot_{1,2}$), $J_1 = J_2$ = 8.7 Hz, 1H], 5.22 [ABq (Rot_1), J = 16.4 Hz, Rot_2 appears as a br s at 5.10 ppm, 2H], 5.20 (s, 2H), 4.50−3.65 (m, 5H), 3.63−3.43 (m, 5H), 3.41−3.21 (m, 5H), 3.20−3.14 [2 × s ($Rot_{1,2}$),3H], 1.41−1.27 [2 × s ($Rot_{1,2}$),9H]; ^{13}C $NMR_{major\ rotamer}$ (DMSO-d_6, 75 MHz) δ 28.6, 44.5, 49.3, 58.5, 63.4, 66.7, 70.0, 70.2, 70.4, 71.0, 71.7, 78.2, 78.6, 123.3, 126.8, 128.3, 128.4, 128.8, 136.8, 145.7, 149.7, 151.8, 152.9, 155.7, 167.8; HRMS (ESI/$MS_{m/z}$) M calcd for $C_{30}H_{40}N_7O_{10}Na_2$ 704.2632, found 704.2620.

*Data for Boc-(2-(2-methoxyethoxy)ethyl)-L-serine guanine(Cbz) monomer (**7c**):* ^{1}H NMR (DMSO-d_6, 300 MHz) δ 7.78−7.72 [2 × s ($Rot_{1,2}$), 1H], 7.48−7.23 (m, 5H), 7.00−6.61 [2 × d ($Rot_{1,2}$), $J_1 = J_2$ = 8.6 Hz, 1H], 5.22−5.19 [2 × s ($Rot_{1,2}$), 2H], 5.03−4.84 [ABq (Rot_1), J = 17.3 Hz, br s (Rot_2), 2H], 3.98−3.62 (m, 4H), 3.59−3.40 (m, 7H), 3.41−3.23 (m, 4H), 3.22−3.12 [2 × s ($Rot_{1,2}$), 3H], 1.35−1.31 [2 × s ($Rot_{1,2}$), 9H]; ^{13}C $NMR_{major\ rotamer}$ (DMSO-d_6, 75 MHz) δ 28.6, 44.4, 49.3, 52.7, 58.5, 67.4, 70.0, 70.1, 70.2, 70.4, 71.0, 71.7, 78.2, 119.4, 128.4, 128.5, 128.6, 128.9, 136.1, 140.8, 147.9, 150.2, 155.7, 166.7, 167.9, 171.9; HRMS (ESI/$MS_{m/z}$) M calcd for $C_{30}H_{40}N_7O_{11}Na_2$ 720.2581, found 720.2581.

*Data for Boc-(2-(2-methoxyethoxy)ethyl)-L-serine cytosine(Cbz) monomer (**7d**):* ^{1}H NMR (DMSO-d_6, 300 MHz) δ 7.84 (d, J = 7.2 Hz, 1H), 7.43−7.24 (m, 5H), 7.01−6.93 [2 × d ($Rot_{1,2}$), $J_1 = J_2$ = 7.3 Hz, 1H], 6.87−6.58 [2 × d ($Rot_{1,2}$), $J_1 = J_2$ = 8.73 Hz, 1H], 5.17 (s, 2H), 4.9−4.5 [ABq (Rot_1), J = 15.8 Hz, br s (Rot_2), 2H], 4.01−3.61 (m, 3H), 3.58−3.43 (m, 7H), 3.43−3.23 (m, 5H), 3.22−3.16 [2 × s ($Rot_{1,2}$), 3H], 1.35 (s, 9H); ^{13}C $NMR_{major\ rotamer}$ (DMSO-d_6, 75 MHz) δ 28.1, 48.6, 48.9, 49.7, 52.2, 58.0, 66.4, 69.5, 69.7, 69.8, 70.4, 71.2, 77.8, 94.0, 127.9, 128.1, 128.4, 135.9, 150.9, 153.1, 155.1, 155.2, 163.0, 167.8, 172.2; HRMS (ESI/$MS_{m/z}$) M calcd for $C_{29}H_{40}N_5O_{11}Na_2$ 680.2520, found 680.2546.

Determination of Optical Purities. *A General Procedure for Preparing MTPA Derivatives. Compound **8**.* To a stirred, cold solution of **2** (100 mg) in DCM (5 mL) was added 5 mL of TFA/*m*-cresol solution (95:5). The ice bath was removed, and the reaction mixture was stirred at room temperature overnight. The solvent was evaporated under reduced pressure and triturated with diethyl ether (3 × 5 mL). The remaining residue was dried under high vacuum overnight and used in the next coupling step without further purification. The crude residue was dissolved in DCM (5 mL) and chilled at 0 °C. DIPEA (2.0 equiv) and (*S*)-(+)-α-methoxy-α-(trifluoromethyl)phenylacetyl chloride (MTPA-Cl; 1.1 equiv) were added, and the reaction mixture was stirred at room temperature overnight. After completion, the solution was diluted with DCM and washed with water (2 × 10 mL) and then brine solution. The organic layer was dried on Na_2SO_4, concentrated under reduced pressure, and purified by column chromatography. Compounds **9** and **10** were prepared the same way.

*Data for 3-[2-(2-methoxyethoxy)ethoxy]-2-[(3,3,3-trifluoro-2-methoxy-2-phenylpropionyl)amino]propionic acid (**8**):* ^{1}H NMR (300 MHz, $CDCl_3$) δ 7.78 (br s, 1H), 7.56 (m, 2H), 7.37 (m, 3H), 4.47 (m, 1H), 4.03−3.7 (m, 2H), 3.68−3.45 (m, 8H), 3.40 (s, 3H), 3.30 (s, 3H); ^{13}C NMR (DMSO-d_6, 75 MHz) δ 42.7, 52.1, 54.8, 55.6, 57.9, 60.1, 68.9, 69.5, 69.6, 71.2, 72.3, 83.8, 127.2, 127.5, 128.1, 129.4, 165.3, 174.7; HRMS (ESI/$MS_{m/z}$) M calcd for $C_{18}H_{24}F_3NO_7Na$ 446.1403, found 446.1359; ^{19}F NMR (300 MHz, $CDCl_3$) δ −69.58 (s, L-stereomer), −69.24 (s, D-stereomer).

*Data for 3,3,3-trifluoro-N-{2-hydroxy-1-[[2-(2-methoxyethoxy)-ethoxy]methyl]ethyl}-2-methoxy-2-phenylpropionamide (**9**):* ^{1}H NMR (300 MHz, $CDCl_3$) δ 7.55 (m, 2H), 7.44 (br s, 1H), 7.40 (m, 3H), 4.13 (m, 1H), 3.83 (m, 1H), 3.70−3.60 (m, 9H), 3.54 (m, 2H), 3.41(m, 3H), 3.37 (s, 3H), 3.07 (br s, 1H); ^{13}C NMR (CDCl3, 75 MHz) δ 50.5, 54.3, 58.4, 62.2, 69.8, 69.89, 69.9, 70.2, 71.3, 72.1, 83.4, 121.4, 125.2, 127.2, 128.0, 128.9, 132.0, 165.9; HRMS (ESI/$MS_{m/z}$) M calcd for $C_{18}H_{26}F_3NO_6Na$ 432.1610 found 432. 1595; ^{19}F NMR (300 MHz, $CDCl_3$) δ −69.43 (s, L-stereomer), −69.33 (s, D-stereomer).

*Data for {[3-[2-(2-methoxyethoxy)ethoxy]-2-[(3,3,3-trifluoro-2-methoxy-2-phenylpropionyl)amino]propyl][2-thyminylacetyl]amino}-acetic acid (**10**):* ^{1}H NMR (300 MHz, DMSO-d_6) δ 11.22 (br s, 1H), 8.33 and 8.25 (2 × d, J = 8.5 Hz, 1H), 7.54−7.35 (m, 5H), 7.09 and 6.96 (2 × s,1H), 4.52−4.26 (ABq, J = 16.8 Hz, 2H), 4.26−4.16 (m, 1H) 3.6−3.34 (m, 16H), 3.21 and 3.20 (2 × s, 3H), 3.10 (ABq, J = 14.0 Hz, 2H), 1.70 and 1.68 (2 × s, 3H); ^{13}C $NMR_{major\ rotamer}$ (DMSO-d_6, 75 MHz) δ 11.8, 47.5, 48.0, 48.4, 52.2, 54.8, 58.0, 69.2, 69.5, 69.6, 69.9, 71.2, 83.7, 107.9, 127.0, 127.2, 128.3, 129.3, 133.3, 142.0, 151.0, 164.3, 165.3, 168.2, 171.6; HRMS (ESI/$MS_{m/z}$) M calcd for $C_{27}H_{35}F_3N_4O_{10}Na$ 655.2305 found 655.2299; ^{19}F NMR (300 MHz, $CDCl_3$) δ −68.80 and −68.95 (s, L-stereomer), −68.70 (s, D-stereomer).

Oligomer Synthesis. Unmodified, Boc-protected PNA monomers were purchased from a commercial supplier (they are no longer available). The oligomers were synthesized on MBHA resin according to the published protocol.[87] Upon completion of the last monomer coupling, the oligomers were cleaved from the resin (and the protecting groups were simultaneously removed) by immersing the resin in a cocktail containing *m*-cresol/thioanisole/TFA/TFMSA (150/150/900/300 μL—for 100 mg of resin) for 2 h. The crude mixture was eluted and precipitated in ethyl ether, dissolved in a water/acetonitrile mixture (80:20), purified by reversed-phase HPLC, and characterized by MALDI-TOF mass spectrometry. A solution of α-cyano-4-hydroxycinnamic acid (10 mg of α-cyano-4-hydroxycinnamic acid in 500 mL of water with 0.1% TFA and 500 mL of acetonitrile with 0.1% TFA) was used as the matrix for MALDI-TOF analysis. Concentrations of the oligomers were determined by UV absorption at 260 nm at 90 °C in water using the following extinction coefficients: 13 700 M^{-1} cm^{-1} (A), 11 700 M^{-1} cm^{-1} (G), 6600 M^{-1} cm^{-1} (C), and 8600 M^{-1} cm^{-1} (T).

Circular Dichroism (CD). All CD data were recorded at room temperature unless otherwise stated. All spectra represent an average of at least 15 scans, recorded from 320 to 200 nm at the rate of 100 nm/min. A 1 cm path length cuvette was used, and the temperature was maintained at 22 °C. All spectra were processed using Origin software, baseline subtracted and, unless otherwise noted, smoothed using a five-point adjacent averaging algorithm.

Melting Temperature (T_m). All hybridization experiments were performed by measuring the change in the absorbance at 260 nm as a function of temperature. All samples were prepared by mixing a stoichiometric amount of each strand (5 μM) in a 10 mM sodium phosphate at pH 7.4 and annealed prior to each measurement. The recorded spectra were smoothed using a five-point adjacent averaging algorithm unless otherwise specified. The melting transitions were determined by taking the first derivative of the absorbance−temperature profile.

Thermodynamic Analysis. Thermodynamic parameters were determined from concentration-dependent T_m measurements following van't Hoff analysis.[95] $\Delta H°$ and $\Delta S°$ were obtained from a plot of $1/T_m$ (K^{-1}) vs ln C_T, where C_T is the total strand concentration. $\Delta H°$ was obtained from the slope of the plot, which should be a linear function, using the relationship slope = $(n - 1)R/\Delta H$, where n is the molecularity of the association interaction (in this case, n = 2) and R is the gas constant (R = 8.314 J/(mol·K)). $\Delta S°$ was determined from the y intercept (ln C_T = 0), where for a non-self-complementary oligonucleotide the following relationship stands: slope = $[\Delta S° - (n - 1)R \ln 2n]/$

dx.doi.org/10.1021/jo200482d |*J. Org. Chem.* 2011, 76, 5614–5627

$\Delta H°$. $\Delta G°$ was calculated at 298.15 K using the equation $\Delta G° = \Delta H° - T\Delta S°$ and K using the equation $\Delta G° = -RT \ln K$.

SPR Analysis. DNA and PNA concentrations were calculated by measuring sample absorbance at 260 nm and 90 °C. At this temperature the bases are unstacked, resulting in the extinction coefficient of the oligomer being equal to the sum of the extinction coefficients of its bases. The DNA extinction coefficients were obtained from the literature, while the PNA extinction coefficients were provided by the commercial supplier.

SPR experiments were conducted on a Biacore T100 with a four-channel carboxymethylated dextran-coated gold sensor chip (CM5) at 25 °C. Approximately 6300 response units (RU) of streptavidin was immobilized on the chip's surface at a flow rate of 5 μL/min using standard *N*-hydroxysuccinimide/1-ethyl-3-[3-(dimethylamino)propyl]-carbodiimide hydrochloride (NHS/EDC) coupling followed by capping with ethanolamine. Then 100 RU of 5′-biotinylated DNA was attached to the chip via noncovalent capture at a flow rate of 2 μL/min and a sample concentration of 25 nM. HBS-EP (0.01 M HEPES, 0.15 M NaCl, 3 mM EDTA, and 0.005% Surfactant P-20, pH 7.4) was used as the running buffer for both the streptavidin and biotinylated DNA immobilizations.

Kinetic information was obtained from the SPR studies by flowing a dilution series (10−50 nM in 10 nM increments) of PNA across the chip. All samples were run in triplicate at a flow rate of 50 μL/min with a running buffer consisting of 10 mM sodium phosphate, pH 7.4, 100 mM NaCl, 0.1 mM EDTA, and 0.005% Surfactant P-20. The chip was regenerated with two 30 s pulses of 10 mM NaOH/1 M NaCl. Buffer injections were conducted before each sample injection to flush any lingering regeneration solution. All samples were reference corrected to account for nonspecific binding by subtracting off the signal resulting from flowing sample over a streptavidin-coated (i.e., no DNA) flow cell. Kinetic constants were calculated using a 1:1 binding global fit model in Biacore T100 Evaluation Software.

Solubility. A saturated solution was prepared for each oligomer by dissolving the dried pellet in a minimum amount of water so that after, heating at 95 °C for 5 min and thorough mixing, undissolved material still remained in the solution. The samples were centrifuged at 12000*g* for 5 min. The concentrations of the saturated solutions were determined by measuring the UV absorption at 260 nm following a serial dilution.

Self-Aggregation. Samples containing different concentrations of the PNA1X−PNA1Y or PNA4X−PNA4Y pair at equimolar ratios were prepared in 10 mM sodium phosphate buffer at pH 7.4. The samples were allowed to equilibrate for 1 h. The fluorescence spectrum of each sample was recorded at room temperature on a fluorescence spectrometer from 490 to 700 nm upon excitation at 475 nm (FITC). All spectra were subtracted from the buffer baseline and smoothed using a five-point adjacent averaging algorithm on the Origin software. FRET efficiencies were determined using the relationship $E = 1 - F'_D/F_D$, where F'_D and F_D are the fluorescence intensities with and without the acceptor, respectively. The donor in this case is FITC (X). For the PNA1X−PNA1Y pair, $F'_D = F'_{PNA1X-PNA1Y}$ and $F_D = F_{PNA1X}$, and for the PNA4X−PNA4Y pair, $F'_D = F'_{PNA4X-PNA4Y}$ and $F_D = F_{PNA4X}$, at the respective concentration.

Off-Target Binding. A PCR product, 171 bp in length (0.4 μM), was separately incubated with 4, 10, and 20 μM PNA6 and PNA10 in sodium phosphate buffer at 37 °C for 16 h. Following incubation, the samples were separated on nondenaturing polyacrylamide gel and stained with SYBR-Gold. The gel was washed three times with 1× TBE buffer and imaged using the BioDoc-It gel documentation system.

■ ASSOCIATED CONTENT

Supporting Information. UV absorption spectra of PNA11−13, ^{1}H and ^{13}C NMR spectra of compounds **1**−**10**, HPLC and MALDI-TOF MS spectra of PNA1−10, UV melting curves of PNA5−DNA and PNA5−RNA duplexes containing perfectly matched and single-base-mismatched targets, CD melting curves of PNA2−5, and SPR sensorgrams and kinetic fits for PNA1−5. This material is available free of charge via the Internet at http://pubs.acs.org.

■ AUTHOR INFORMATION

Corresponding Author
*E-mail: dly@andrew.cmu.edu.

■ ACKNOWLEDGMENT

Financial support for this work was provided by the National Institutes of Health (Grant GM076251) and the National Science Foundation (NSF; Grant CHE-1012467) to D.H.L. SPR instrumentation was purchased with support from NSF Major Research Instrumentaion Award 0821296. K.J.Z. gratefully acknowledges support from Department of Defense, Air Force Office of Scientific Research, National Defense Science and Engineering Graduate Fellowship 32 CFR168a.

■ REFERENCES

(1) Nielsen, P. E.; Egholm, M.; Berg, R. H.; Buchardt, O. *Science* **1991**, *254*, 1497–1500.
(2) Egholm, M.; Buchardt, O.; Christensen, L.; Behrens, C.; Freier, S. M.; Driver, D. A.; Berg, R. H.; Kim, S. K.; Norden, B.; Nielsen, P. E. *Nature* **1993**, *365*, 566–568.
(3) Nielsen, P. E. *Acc. Chem. Res.* **1999**, *32*, 624–630.
(4) Bentin, T.; Larsen, H. J.; Nielsen, P. E. *Biochemistry* **2003**, *42*, 13987–13995.
(5) Kaihatsu, K.; Shah, R. H.; Zhao, X.; Corey, D. R. *Biochemistry* **2003**, *42*, 13996–14003.
(6) Tomac, S.; Sarkar, M.; Ratilainen, T.; Wittung, P.; Nielsen, P. E.; Norden, B.; Graeslund, A. *J. Am. Chem. Soc.* **1996**, *118*, 5544–5552.
(7) Ratilainen, T.; Holmen, A.; Tuite, E.; Nielsen, P. E.; Norden, B. *Biochemistry* **2000**, *39*, 7781–7791.
(8) Menchise, V.; De Simone, G.; Tedeschi, T.; Corradini, R.; Sforza, S.; Marchelli, R.; Capasso, D.; Saviano, M.; Pedone, C. *Proc. Natl. Acad. Sci. U.S.A.* **2003**, *100*, 12021–12026.
(9) Rasmussen, H.; Kastrup, J. S.; Nielsen, J. N.; Nielsen, J. M.; Nielsen, P. E. *Nat. Struct. Biol.* **1997**, *4*, 98–101.
(10) Haaima, G.; Rasmussen, H.; Schmidt, G.; Jensen, D. K.; Kastrup, J. S.; Stafshede, P. W.; Norden, B.; Buchardt, O.; Nielsen, P. E. *New J. Chem.* **1999**, *23*, 833–840.
(11) Eldrup, A. B.; Nielsen, B. B.; Haaima, G.; Rasmussen, H.; Kastrup, J. S.; Christensen, C.; Nielsen, P. E. *Eur. J. Org. Chem.* **2001**, 1781–1790.
(12) Demidov, V. V.; Potaman, V. N.; Frank-Kamenetskii, M. D.; Egholm, M.; Buchard, O.; Sonnichsen, S. H.; Nielsen, P. E. *Biochem. Pharmacol.* **1994**, *48*, 1310–1313.
(13) Dueholm, K. L.; Egholm, M.; Behrens, C.; Christensen, L.; Hansen, H. F.; Vulpius, T.; Petersen, K. H.; Berg, R. H.; Nielsen, P. E.; Buchardt, O. *J. Org. Chem.* **1994**, *59*, 5767–5773.
(14) Thomson, S. A.; Josey, J. A.; Cadilla, R.; Gaul, M. D.; Hassman, C. F.; Luzzio, M. J.; Pipe, A. J.; Reed, K. L.; Ricca, D. J.; Wiethe, R. W.; Noble, S. A. *Tetrahedron* **1995**, *51*, 6179–6194.
(15) Beck, F.; Nielsen, P. E. *Artificial DNA: Methods and Applications*; CRC Press: Boca Raton, FL, 2003; pp 91−114.
(16) Ray, A.; Norden, B. *FASEB J.* **2000**, *14*, 1041–1060.
(17) Nielsen, P. E. *Mol. Biotechnol.* **2004**, *26*, 233–248.
(18) Veselkov, A. G.; Demidov, V. V.; Frank-Kamenetskii, M. D.; Nielsen, P. E. *Nature* **1996**, *379*, 214.
(19) Komiyama, M.; Aiba, Y.; Yamamoto, Y.; Sumaoka, J. *Nat. Protoc.* **2008**, *3*, 655–622.

(20) Chin, J. Y.; Kuan, J. Y.; Lonkar, P. S.; Krause, D. S.; Seidman, M. M.; Peterson, K. R.; Nielsen, P. E.; Kole, R.; Glazer, P. M. *Proc. Natl. Acad. Sci. U.S.A.* **2008**, *105*, 13514–13519.
(21) Singer, A.; Wanunu, M.; Morrison, W.; Kuhn, H.; Frank-Kamenetskii, M.; Meller, A. *Nano Lett.* **2010**, *10*, 738–742.
(22) Mollegaard, N. E.; Buchardt, O.; Egholm, M.; Nielsen, P. E. *Proc. Natl. Acad. Sci. U.S.A.* **1994**, *91*, 3892–3895.
(23) Janowski, B. A.; Kaihatsu, K.; Huffman, K. E.; Schwartz, J. C.; Ram, R.; Hardy, D.; Mendelson, C. R.; Corey, D. R. *Nat. Chem. Biol.* **2005**, *1*, 210–215.
(24) Winssinger, N.; Ficarro, S.; Schultz, P. G.; Harris, J. L. *Proc. Natl. Acad. Sci. U.S.A.* **2002**, *99*, 11139–11144.
(25) Debaene, F.; Da Silva, J. A.; Pianowski, Z.; Duran, F. J.; Winssinger, N. *Tetrahedron* **2007**, *63*, 6577–6586.
(26) Bruno, Y.; Birnbaum, M. E.; Kleiner, R. E.; Liu, D. R. *Nat. Chem. Biol.* **2010**, *6*, 148–155.
(27) Ura, Y.; Beierle, J. M.; Leman, L. J.; Orgel, L. E.; Ghadiri, M. R. *Science* **2009**, *325*, 73–77.
(28) Myers, C. P.; Williams, M. E. *Coord. Chem. Rev.* **2010**, *254*, 2416–2428.
(29) Chakrabarti, R.; Klibanov, A. M. *J. Am. Chem. Soc.* **2003**, *125*, 12531–12540.
(30) Janssen, P. G. A.; Meeuwenoord, N.; van der Marel, G.; Jabbari-Farouji, S.; van der Schoot, P.; Surin, M.; Tomovic, Z.; Meijer, E. W.; Schenning, A. P. H. J. *Chem. Commun.* **2010**, *46*, 109–111.
(31) Riaz, U.; Ahmad, S.; Ashraf, S. M. *J. Nanopart. Res.* **2008**, *10*, 1209–1214.
(32) Popescu, D. L.; Parolin, T. J.; Achim, C. *J. Am. Chem. Soc.* **2003**, *125*, 6354–6355.
(33) Braasch, D. A.; Corey, D. R. *Methods* **2001**, *23*, 97–107.
(34) Tackett, A. J.; Corey, D. R.; Raney, K. D. *Nucleic Acids Res.* **2002**, *30*, 950–957.
(35) Masuko, M. *Nucleic Acids Res. Suppl.* **2003**, 145–146.
(36) Cattani-Scholz, A.; Pedone, D.; Blobner, F.; Abstreiter, G.; Schwartz, J.; Tornow, M.; Andruzzi, L. *Biomacromolecules* **2009**, *10*, 489–496.
(37) Egholm, M.; Buchardt, O.; Nielsen, P. E.; Berg, R. H. *J. Am. Chem. Soc.* **1992**, *114*, 1895–1897.
(38) Haaima, G.; Lohse, A.; Buchardt, O.; Nielsen, P. E. *Angew. Chem., Int. Ed. Engl.* **1996**, *35*, 1939–1941.
(39) Sforza, S.; Tedeschi, T.; Corradini, R.; Marchelli, R. *Eur. J. Org. Chem.* **2007**, 5879–5885.
(40) Boyarskaya, N. P.; Kirillova, Y. G.; Stotland, E. A.; Prokhorov, D. I.; Zvonkova, E. N.; Shvets, V. I. *Dokl. Chem. (Transl. of Dokl. Akad. Nauk)* **2006**, *408*, 57–60.
(41) Gildea, B. D.; Casey, S.; MacNeill, J.; Perry-O'Keefe, H.; Sorensen, D.; Coull, J. M. *Tetrahedron Lett.* **1998**, *39*, 7255–7258.
(42) Hudson, R. H. E.; Liu, Y.; Wojciechowski, F. *Can. J. Chem.* **2007**, *85*, 302–312.
(43) Peyman, A.; Uhlmann, E.; Wagner, K.; Augustin, S.; Breipohl, G.; Will, D. W.; Schafer, A.; Wallmeier, H. *Angew. Chem., Int. Ed. Engl.* **1996**, *35*, 2636–2638.
(44) Efimov, V. A.; Choob, M. V.; Buryakova, A. A.; Kalinkina, A. L.; Chakhmakhcheva, O. G. *Nucleic Acids Res.* **1998**, *26*, 566–575.
(45) Bonora, G. M.; Drioli, S.; Ballico, M.; Faccini, A.; Corradini, R.; Cogoi, S.; Xodo, L. *Nucleosides, Nucleotides, Nucleic Acids* **2007**, *26*, 661–664.
(46) Petersen, K. H.; Jensen, D. K.; Egholm, M.; Nielsen, P. E.; Buchardt, O. *Bioorg. Med. Chem. Lett.* **1995**, *5*, 1119–1124.
(47) Bergmann, F.; Bannwarth, W.; Tam, S. *Tetrahedron Lett.* **1995**, *36*, 6823–6826.
(48) Uhlmann, E.; Will, D. W.; Breipohl, G.; Langner, D.; Ryte, A. *Angew. Chem., Int. Ed. Engl.* **1996**, *35*, 2632–2635.
(49) Finn, P. J.; Gibson, N. J.; Fallon, R.; Hamilton, A.; Brown, T. *Nucleic Acids Res.* **1996**, *24*, 3357–3363.
(50) vander Laan, A. C.; Brill, R.; Kuimelis, R. G.; KuylYeheskiely, E.; vanBoom, J. H.; Andrus, A.; Vinayak, R. *Tetrahedron Lett.* **1997**, *38*, 2249–2252.
(51) Kuwahara, M.; Arimitsu, M.; Sisido, M. *J. Am. Chem. Soc.* **1999**, *121*, 256–257.
(52) Harris, J. M.; Chess, R. B. *Nat. Rev. Drug Discovery* **2003**, *2*, 214–221.
(53) Veronese, F. M.; Pasut, G. *Drug. Discovery Today* **2005**, *10*, 1451–1458.
(54) Knop, K.; Hoogenboom, R.; Fischer, D.; Schubert, U. S. *Angew. Chem., Int. Ed.* **2010**, *49*, 6288–6308.
(55) Roberts, M. J.; Benley, M. D.; Harris, J. M. *Adv. Drug. Delivery Rev.* **2002**, *54*, 459–476.
(56) Wang, Y.; Chang, F.; Zhang, Y.; Liu, N.; Liu, G.; Gupta, S.; Rusckowski, M.; Hnatowich, D. J. *Bioconjugate Chem.* **2001**, *12*, 807–816.
(57) Rapozzi, V.; Cogoi, S.; Spessotto, P.; Risso, A.; Bonora, G. M.; Quadrifoglio, F.; Xodo, L. E. *Biochemistry* **2002**, *41*, 502–510.
(58) Bonora, G. M. *J. Bioact. Compat. Polym.* **2002**, *17*, 375389.
(59) Zhao, H.; Greenwald, R. B.; Reddy, P.; Xia, J.; Peng, P. *Bioconjugate Chem.* **2005**, *16*, 758–766.
(60) Liu, B.; Burdine, L.; Kodadek, T. *J. Am. Chem. Soc.* **2006**, *128*, 15228–15235.
(61) Kikkeri, R.; Lepenies, B.; Adibekian, A.; Laurino, P.; Seeberger, P. H. *J. Am. Chem. Soc.* **2009**, *131*, 2110–2112.
(62) Konig, H. M.; Gorelik, T.; Kolb, U.; Kilbinger, A. F. M. *J. Am. Chem. Soc.* **2006**, *129*, 704–708.
(63) Gopin, A.; Ebner, S.; Attali, B.; Shabat, D. *Bioconjugate Chem.* **2006**, *17*, 1432–1440.
(64) Xiong, S.; Li, H.; Yu, B.; Wu, J.; Lee, R. J. *J. Pharm. Sci.* **2010**, *99*, 5011–5018.
(65) Zhao, H.; Duong, H. H. P.; Yung, L. Y. L. *Macromol. Rapid Commun.* **2010**, *31*, 1163–1169.
(66) Nagahori, N.; Abe, M.; Nishimura, S.-I. *Biochemistry* **2009**, *48*, 583–594.
(67) Li, J.; Chen, Y.-C.; Tseng, Y.-C.; Mozumdar, S.; Huang, L. *J. Controlled Release* **2010**, *142*, 416–421.
(68) Arnaud, A.; Belleney, J.; Boue, F.; Bouteiller, L.; Carrot, G.; Wintgens, V. *Angew. Chem., Int. Ed.* **2004**, *43*, 1718–1721.
(69) Dragulescu-Andrasi, A.; Rapireddy, S.; Frezza, B. M.; Gayathri, C.; Gil, R. R.; Ly, D. H. *J. Am. Chem. Soc.* **2006**, *128*, 10258–10267.
(70) Rapireddy, S.; He, G.; Roy, S.; Armitage, B. A.; Ly, D. H. *J. Am. Chem. Soc.* **2007**, *129*, 15596–15600.
(71) Chenna, V.; Rapireddy, S.; Sahu, B.; Ausin, C.; Pedroso, E.; Ly, D. H. *ChemBioChem* **2008**, *9*, 2388–2391.
(72) Sahu, B.; Chenna, V.; Lathrop, K. L.; Thomas, S. M.; Zon, G.; Livak, K. J.; Ly, D. H. *J. Org. Chem.* **2009**, *74*, 1509–1516.
(73) Yeh, J. I.; Shivachev, B.; Rapireddy, S.; Crawford, M. J.; Gil, R. R.; Du, S.; Madrid, M.; Ly, D. H. *J. Am. Chem. Soc.* **2010**, *132*, 10717–10727.
(74) Kosynkina, L.; Wang, W.; Liang, T. C. *Tetrahedron Lett.* **1994**, *35*, 5173–5176.
(75) Falkiewicz, B.; Kowalska, K.; Kolodziejczyk, A. S.; Wisniewski, K.; Lankiewicz, L. *Nucleosides Nucleotides* **1999**, *18*, 353–361.
(76) Wu, Y.; Xu, J. C. *Tetrahedron* **2001**, *57*, 8107–8113.
(77) Tedeschi, T.; Sforza, S.; Corradini, R.; Marchelli, R. *Tetrahedron Lett.* **2005**, *46*, 8395–8399.
(78) Dose, C.; Seitz, O. *Org. Lett.* **2005**, *7*, 4365–4368.
(79) Englund, E. A.; Appella, D. H. *Org. Lett.* **2005**, *7*, 3465–3467.
(80) Englund, E. A.; Appella, D. H. *Angew. Chem., Int. Ed.* **2007**, *46*, 1414–1418.
(81) He, G.; Rapireddy, S.; Bahal, R.; Sahu, B.; Ly, D. H. *J. Am. Chem. Soc.* **2009**, *131*, 12088–12090.
(82) Fukuyama, T.; Cheung, M.; Jow, C.-K.; Hidai, Y.; Kan, T. *Tetrahedron Lett.* **1997**, *38*, 5831–5834.
(83) Debaene, F.; Winssinger, N. *Org. Lett.* **2003**, *5*, 4445–4447.
(84) Corradini, R.; Di Silvestro, G.; Sforza, S.; Palla, G.; Dossena, A.; Nielsen, P. E.; Marchelli, R. *Tetrahedron: Asymmetry* **1999**, *10*, 2063–2066.
(85) Seco, J. M.; Quinoa, E.; Riguera, R. *Chem. Rev.* **2004**, *104*, 17–117.
(86) Rodriguez, M.; Llinares, M.; Doulut, S.; Martinez, J. *Tetrahedron Lett.* **1991**, *32*, 923–926.

(87) Christensen, L.; Fitzpatrick, R.; Gildea, B.; Petersen, K. H.; Hansen, H. F.; Koch, T.; Egholm, M.; Buchardt, O.; Nielsen, P. E.; Coull, J.; Berg, R. H. *J. Pept. Sci.* **1995**, *1*, 175–183.
(88) Tedeschi, T.; Corradini, R.; Marchelli, R.; Pushl, A.; Nielsen, P. E. *Tetrahedron: Asymmetry* **2002**, *13*, 1629–1636.
(89) Sen, S.; Nilsson, L. *J. Am. Chem. Soc.* **2001**, *123*, 7414–7422.
(90) Johnson, W. C. *Circular Dichroism: Principles and Applications*; Wiley-VCH: New York, 2000.
(91) Nielsen, E. B.; Schellman, J. A. *J. Phys. Chem.* **1967**, *71*, 2297–2304.
(92) Wittung, P.; Nielsen, P. E.; Buchardt, O.; Egholm, M.; Norden, B. *Nature* **1994**, *368*, 561–563.
(93) Eriksson, M.; Nielsen, P. E. *Nat. Struct. Biol.* **1996**, *3*, 410–413.
(94) Cheatham, T. E. I.; Kollman, P. A. *J. Am. Chem. Soc.* **1997**, *119*, 4805.
(95) Marky, L.; Breslauer, K. J. *Biopolymers* **1987**, *26*, 1601–1620.
(96) Gildea, B. D.; Coull, J. M.; Hyldig-Nielsen, J. J.; Fiandaca, M. J. WO A-9921881, 1999.
(97) Ananthanawat, C.; Vilainvan, T.; Hoven, V.; Su, X. *Biosens. Bioelectron.* **2010**, *25*, 1064–1069.
(98) Lao, A. I.; Su, X.; Aung, K. M. M. *Biosens. Bioelectron.* **2009**, *24*, 1717–1722.
(99) Sawata, S.; Kai, E.; Ikebukuro, K.; Iida, T.; Honda, T.; Karube, I. *Biosens. Bioelectron.* **1999**, *14*, 397–404.
(100) Roy, S.; Tanious, F. A.; Wilson, W. D.; Ly, D. H.; Armitage, B. A. *Biochemistry* **2007**, *46*, 10433–10443.
(101) Lusvarghi, S.; Murphy, C. T.; Roy, S.; Tanious, F. A.; Sacui, I.; Wilson, W.; Ly, D. H.; Armitage, B. A. *J. Am. Chem. Soc.* **2009**, *131*, 18415–18424.